INTEGRATION OF A COLLAGEN-HYDROXYAPATITE SCAFFOLD INTO OSTEOCHONDRAL CYLINDERS FROM BOVINE KNEE JOINTS – AN IN VITRO STUDY

Dissertation

zur Erlangung des akademischen Grades

doctor medicinae (Dr. med.)

vorgelegt dem Rat der Medizinischen Fakultät
der Friedrich-Schiller-Universität Jena

von **Sebastian Walter**

geboren am **25. September 1990** **in** **Apolda**

Gutachter

1. Herr Prof. Dr. med. R. W. Kinne, Exp. Rheumatologie Eisenberg

2. Herr PD Dr. med. M. Lenz, Klinik für Unfallchirurgie Jena

3. Herr Prof. Dr. med. W. Thomas, European Hospital Rom, Italien

Tag der öffentlichen Verteidigung: 22.12.2017

TABLE OF CONTENTS

ABBREVIATIONS AND SI-UNITS

ACT	**Autologous Chondrocyte Transplantation**
AGC	**Aggrecan**
cDNA	**complementary Deoxyribonucleic Acid**
Col 1	**Collagen 1**
Col 2	**Collagen 2**
COMP	**Cartilage Oligomeric Matrix Protein**
CO_2	**Carbon Dioxide**
ECM	**Extracellular Matrix**
ELISA	**Enzyme-Linked ImmunoSorbent Assay**
FBS	**Fetal Bovine Serum**
GAG	**Glycosaminoglycan**
HA	**Hydroxyapatite**
HE	**Hematoxylin Eosin**
H_2O_2	**Hydrogen peroxide**
ITS	**Insulin Transferrin Selenium**
mRNA	**messenger RiboNucleic Acid**
MSC	**Mesenchymal Stem Cell**
OA	**Osteoarthritis**
OAT	**Osteochondral Autologous Transplant**
PCR	**Polymerase Chain Reaction**
pH	**negative logarithm to the base of 10 of the hydrogen ion concentration**
PMMA	**Polymethylmethacrylate**

ROM	**Range of Motion**
qPCR	**quantitative Polymerase Chain Reaction**
rpm	**revolutions per minute**
TBS	**Tris-Buffered Saline**
SEM	**Standard Error of the Mean**
SD	**Standard Deviation**

SI Units

g	**gram**
G	**gravitational constant (6.674×10^{-11} $N\cdot m^2/kg^2$)**
Gy	**Gray (J/kg)**
Hz	**Hertz (s^{-1})**
M	**Molar mass (g/mol)**
m	**meter**
min	**minute**
ml	**millilitre**
N	**Newton ($kg\cdot m/s^2$)**
s	**second**
°C	**degree Celsius**

1 ABSTRACT

Background: Numerous techniques and treatments have been developed to prevent joint cartilage from degenerating or to restore its properties. One of these is MaioRegen® (MR) -a cell-free hybrid scaffold consisting of 3 collagen 1 layers with increasing hydroxyapatite content from the top cartilage to the bottom bone layer-, which demonstrated very promising results in clinical studies.

Material and Methods: A novel model was developed for the investigation of MR's behavior in an in vitro setting. Ring-shaped osteochondral cylinders (outer diameter 8 mm; inner diameter 6 mm) were prepared from fresh bovine knee joints using standardized punches (Arthrex®). Osteochondral autologous transplants (OATs; positive control) or MR scaffolds with a diameter of 6 mm were then inserted into the osteochondral rings and cultured for periods of up to 10 weeks. Histological (HE, Safranin-O, and aggrecan immunohistology), transcriptional (collagen 1, 2, aggrecan, and COMP), biochemical (DMB assay, ELISA for collagen 1, 2 and aggrecan), and biomechanical analyses were performed at the start, as well as after 4, 8 and 10 weeks of in vitro culture.

Results: The culture system remained stable without signs of cell death or necrosis for any tissue component throughout 10 weeks of cell culture. In the OAT group, fibrocartilaginous tissue formation in the osseous part and a complete bridging of the gap between the osseous and transplant was observed after 8 weeks. Despite substantial cell migration into the scaffold, local proteoglycan deposition and significant increases in aggrecan gene expression, in contrast, the MR scaffold progressively dissolved and thus showed decreased biomechanical resistances over time.

Conclusion: The novel model appears suitable for high-throughput investigation of osteochondral regeneration in vitro. The OAT group represents a suitable control for future studies based on its efficient tissue integration in vitro and the similarity of its in vitro and clinical performance. Due to its rapid degradation in vitro and in vivo, the MR scaffold may show limitations in the present in vitro model and in the clinical context of osteochondral regeneration.

2 INTRODUCTION

2.1 Hyaline cartilage

Articular cartilage found in synovial- hydrated joints is called hyaline cartilage. This type of cartilage shows a special stratified structure and molecular arrangement of the extra-cellular matrix (ECM), which is crucial for its smooth and physiological joint function.

2.2 Structure of hyaline cartilage

Hyaline cartilage consists of up to 80% of water. The typical cells of this tissue are chondrocytes, which are present as isolated cells or in multi-cellular chondrones. As cartilage is a bradytrophic tissue, chondrocytes have an anaerobic metabolism (Poole 1997). Supply with oxygen is therefore mainly based on diffusion. This is supported by natural biomechanical pressure that pushes oxygenated synovial fluid into the cartilage (Muir 1995).

The ECM between these cells is highly organized and shows a typical orientation of the collagen fibers (Fig.1). As a result, the cartilage can be subdivided into four layers.

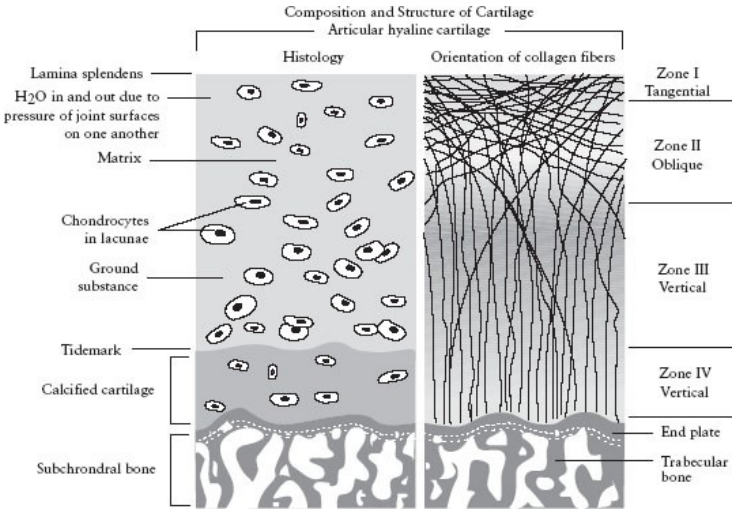

Figure 1: Principal structure of hyaline cartilage, shown by un-blinding the orientation of the collagen fibers and by visualizing shape and distribution of the chondrocytes in the different layers.(Gross 2009)

2.2.1 Surface (tangential) layer

This layer (also known as lamina splendens) represents the part of the cartilage that is closest to the joint space and shows a thickness of 100-300 µm only. Chondrocytes in this layer are flat and spindle-shaped (Poole 1997). In this layer, the concentration of collagen is the highest and cross-linked collagen fibers run parallel to the joint surface. The latter is the reason for the high tensile strength of this layer, which protects the

cartilage from erosive damage through shear forces and tangential stretching (Broom und Marra 1985).

2.2.2 Transitional (oblique) layer

The transitional layer is just beneath the surface layer and above the radiate layer. It shows a high elasticity and accounts for 20 to 70% of the cartilage thickness. From the top to the bottom, the orientation of the cells changes from a tangential to a vertical orientation with respect to the cartilage surface, thus following the changing direction of the collagen fibers (Broom und Marra 1985). Biochemically, this layer is characterized by an increasing concentration of proteoglycans and a decreasing relative concentration of collagen (Poole 1997). Functionally, this results in decreased tensile strength and increased pressure loading capacity.

2.2.3 Radiate (vertical) layer

The radiate layer (also radiate stratum) is situated between the transitional layer and the calcified layer. A clearly detectable edge, called tidemark, is found between the radiate layer and the calcified layer. In this layer, all chondrocytes and collagen fibers are orientated vertically to the cartilage surface and are organized in column-like structures. In this area, the relative concentration of proteoglycans is the highest, while the relative quantity of collagen is decreasing. The maximal concentration of proteoglycans is found at 50 to 70% depth of the overall thickness. This results in a maximal pressure loading capacity of the cartilage in this section (Roth und Mow 1980).

2.2.4 Calcified cartilage

This fourth layer of the cartilage is localized just above the sub-chondral bone (Brighton et al. 1984). In this layer chondrocytes aggregate in small groups, are round-shaped and surrounded by non-calcified lacunae. The special feature of this layer is its ability to regenerate after damage. Although this layer accounts for only 3-9% of the overall thickness of the cartilage, it plays an important role as a potential therapeutic target (Wakitani et al. 1994). At the same time, there is some evidence that progenitor cells that reside in the superficial layer can also contribute to cartilage regeneration (Mesallati et al. 2015).

2.2.5 Extracellular-matrix (ECM)

The ECM of the hyaline cartilage consists of a framework of collagen fibers and the space between the collagen fibers. More than 90% of the collagen fibers consist of collagen type 2, while collagen 1 accounts only for a minor fraction of approximately

10%. The collagen fibers of this framework are organized in parallel and antiparallel fibers (Hedlund et al. 1993). The space between the collagen fibers consists of water, minerals, glycoproteins, and proteoglycans. The most characteristic proteoglycan of hyaline cartilage is the large chondroitin sulfate molecule aggrecan. As a typical proteoglycan, it has a high water binding capacity and is therefore one of the most important proteins for establishing the pressure loading capacity of the joint cartilage (Ulrich-Vinther et al. 2003).

Proteoglycans and collagen fibers build a network with electrostatic interactions, again supporting the enormous pressure loading capacity and tensile strength of hyaline cartilage.

2.3 Functions of hyaline cartilage

There are regionally diverse processes in the cartilage, since proteoglycans have the tendency to accumulate water, whereas collagen fibers limit the expansion of the aggrecan molecules (Shakibaei et al. 2008). These two characteristics are crucial for the pressure loading capacity and the tensile strength of the cartilage. If strain is applied to the cartilage, liquid is pressed out of the cartilaginous tissue and reabsorbed during relaxation. The expelled lubricin-enriched liquid mingles with synovial fluid and contributes to a reduced friction coefficient. Therefore, healthy joints are considered almost frictionless (Jay und Waller 2014).

In the case of joint pathology, a low concentration of proteoglycans and a subsequently reduced swelling leads to an irregular distribution of the mechanical strain. As a consequence, the subchondral bone is more heavily loaded and the cartilage tissue will degenerate.

The opposite effect is observed when defects in the collagen framework lead to a decreased hydrostatic pressure, which results in cartilage edema due to over-absorption of water by proteoglycans (Shakibaei et al. 2008). This complex, balanced system is thus a target of various pathologies, inevitably resulting in the destruction of articular cartilage.

2.4 Acute and traumatic damage

Trauma-derived cartilage damage has a higher incidence among young, sportive and active individuals. Thus, most of the damage results in overstraining peak loads or accidents especially among elite athletes. However, individuals having an insufficient musculature incapable of attenuating the forces of the musculoskeletal system are at

high risk, too. Limited traumatic cartilage damage is not necessarily associated with a loss of cartilage substance and the physiological function of the chondrocytes may remain unimpaired (Buckwalter 1997). Thus, the endogenous regeneration of the cartilage clearly depends on the size and depth of the damage (Fig. 2). There are several different types of defects.

1. Chondral defects. In this case, only cartilaginous tissue is affected and the cartilage is either partially or completely damaged. However, the subchondral bone does not show any lesion. In cases of chondral defects with a diameter of less than 2 mm, endogenous regeneration should be considered as a satisfactory treatment option (Konig und Kirschner 2003).

2. Osteochondral defects. If the full thickness of cartilage and also the subchondral bone are simultaneously damaged, the resulting defect is called an osteochondral defect. As there is no border between bone marrow and cartilage anymore, mesenchymal stem cells (MSC) migrate into the defect and attempt to synthesize novel ECM. However, this ECM shows completely different properties than the cartilaginous ECM, as it contains less proteoglycans and collagen 2, which results in decreased pressure loading capacity and tensile strength. In addition, the damage in the osseous part is not regenerated, but rather replaced by fibrous scar tissue (Bobic 1999). Aseptic osteonecrosis, as in the case of osteochondritis dissecans, represents a special type of osteo-chondral defects. In this case, necrosis develops via a reduced blood supply in the area of insufficiently nourished subchondral bone, which eventually loosens together with its attached cartilage and turns into a painful flake in the joint space (Mubarak und Carroll 1981).

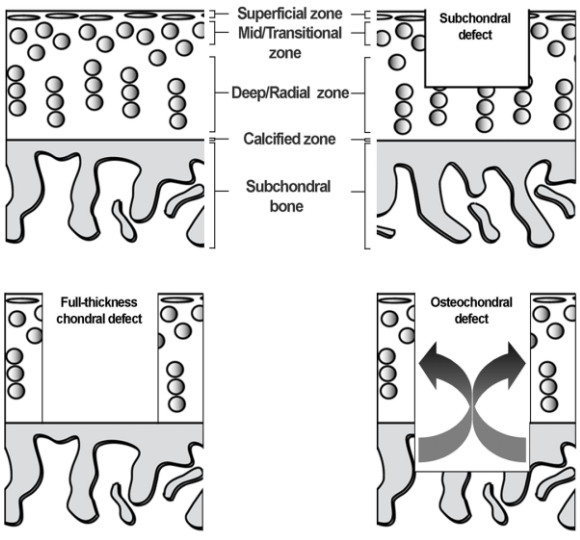

Figure 2: Principally there are two types of cartilage damage: 1. Only the cartilage itself is damaged or 2. The subchondral bone is injured as well. In the second case, MSCs immigrate into the defect area and form fibrocartilaginous tissue (Khan et al. 2008).

2.5 Cartilage degeneration

Age-adapted, physiological adjustments of cartilage metabolism may lead to cartilage degeneration with structural, morphologic, and functional changes. Therefore, the senior population carries an increased risk of suffering from degenerative processes. However, secondary cartilage damage can also appear in young patients, e.g. after infections, improper treatment of biomechanical deviations or impingement of the joint (Bedi et al. 2013).

The end stage of all physiological and pathological cartilage erosion is osteoarthritis (OA)(Hayes et al. 2001, Tuan et al. 2013) with cartilage loss, a dysfunctional range of motion (ROM), and pain upon initiation of movements (Kleemann et al. 2005). OA is one of the most common joint diseases. As a result of previous cartilage damage, chondrocytes change their metabolism, which further contributes to the degeneration (Hart et al. 1999). This results in a reduced thickness of the cartilage. The collagen fibers network cannot withstand large strains any longer and proteoglycans are lost from the matrix. As a result, the pressure loading capacity of the cartilage is impaired, the tissue is progressively damaged and microcracks evolve. In the long run, a complete loss of the cartilage leads to pathological changes of the subchondral bone such as sclerosis, osteophyte formation, and subchondral cysts (Kleemann et al. 2005).

2.6 Treatment strategies

Endoprosthetic total knee or hip arthroplasty is the treatment of choice for OA. However, the implantation of an endoprostheses should be delayed as long as possible, since they have a limited standing time and may thus eventually need to be revised (Goldring und Goldring 2007).

Therefore, early-stage damage of the cartilage has to be treated with care and anticipation. Several established cell-based (e.g. (M)ACT, OAT), cell-free (e.g. bio-engineered scaffolds, cell-free OCT from commercial banks) and stem cell-directed (micro-abrasion, Pridie-drilling) procedures compete for the best clinical outcome (Behery et al. 2014).

2.6.1 Debridement and Lavage

As this cleaning and rinsing technique of the joint only abates the pain and does not repair or regenerate damaged articular cartilage, it has only palliative character (Martinek et al. 2003). Using the mostly arthroscopic joint lavage, digestive, oxidative

enzymes derived from chondro-necrosis are removed. Debridement includes the removal of loose joint bodies and the smoothening of the cartilage surface, also called arthro-cleaning (Schinhan et al. 2012).

2.6.2 Cartilage abrasion

During the arthroscopic examination of a joint, it is a very common strategy to remove worn out layers of the cartilage and “refresh” the surface. This technique is very simple and fast, however it often does not yield a sufficient long-term outcome (Goymann 1999).

2.6.3 Microfracturing

The concept behind this technique (sometimes referred to as Pridie-Drilling) is to enable mesenchymal stem cells to migrate into the damaged cartilage, to differentiate in this location, and to build new cartilaginous tissue. This technique has to be used with caution, as the replacing tissue often does not exactly match the properties and structure of the original cartilage, but rather represents fibrocartilaginous scar tissue (Oussedik et al. 2015). Considering the presence of progenitor cells in the superficial layer of the cartilage and their theoretical potential to form hyaline cartilage like structures, the contribution of this technique to an improved cartilage regeneration has also been questioned (Mesallati et al. 2015).

2.6.4 Osteochondral autologous transplant (OAT)

An osteochondral autologous graft of the size of the defect is harvested from a region of the joint that is less exposed to mechanical strains than the site of the original defect. Then the graft is inserted into the defect by the press-fit technique. One advantage of this method is a very good healing rate at the site of insertion. However, damage is intentionally caused in another joint area and the respective tidemarks of graft and defect are not always perfectly aligned (Lynch et al. 2015).

Figure 3: This scheme demonstrates the procedure of an OAT: First, an appropriate graft is harvested from a peripheral zone of the joint and then implanted at the site of the defect after preparing the recipient site in order to match the height of the graft (Fiedler 2014).

2.6.5 (Matrix-associated) autologous chondrocyte transplantation (M) ACT

In a first intervention, cartilage is arthroscopically harvested from the joint in an area less exposed to mechanical strain. Chondrocytes are then enzymatically liberated from the extracellular matrix and cultured for a period of 4 weeks. After this time, replicated chondrocytes are implanted into the site of damage. This is either done by placing tibial periosteum above the cartilage defect and fixing it with fibrin and injecting the chondrocytes into the resulting chamber or, alternatively, by seeding the cells onto a scaffold (matrix), which is subsequently inserted into the defect. This technique has demonstrated very good clinical results in several studies (Gillogly und Wheeler 2015, Gobbi et al. 2015), especially when treating defects with a diameter larger than 4 cm². Besides the size of the defect area, the location of the defect is a determining factor for the outcome of this technique. When repairing defects on the tibia, the patella or on multiple sites of the knee joint, clinical outcomes are not as good as for defects on the femur. Another pitfall of this cost-intensive procedure is that it requires two interventions (Dewan et al. 2014).

Due to the immuno-evasive properties of cartilage, it is a tissue that may be suitable to a) be banked (in analogy to bone tissue) and b) to be transplanted as a xenograft in one-step operations. This would tremendously contribute to the practicability of this technique.

2.6.6 Tissue-engineered scaffolds

Hyaline cartilage is a bradytrophic tissue and endogenous regeneration of large defects normally results in fibrocartilaginous tissue formation (Triche und Mandelbaum 2013). This is aggravated by the fact that cartilage damage is very common and

regularly leads to the development of OA (Demoor et al. 2014). As a consequence, current research focuses on the improvement of established treatment strategies and the development of new treatment approaches in tissue engineering (Mollon et al. 2013, Tuan et al. 2013). Tissue-engineered scaffolds are designed to imitate the structure of the cartilage in order to support chondrocyte migration into the tissue and the formation of high-quality hyaline cartilage. There is some evidence for good clinical outcomes when using such scaffolds, which stimulates further extensive research in this field (Lim et al. 2014).

The advantages of the cell-free approaches are rapid commercial availability, convenience in handling and a one-time operation procedure. In addition, there is no need for autologous donor sites or tissue donors.

One type of such cell-free constructs is a three-layer, stratified scaffold (MaioRegen®, Finceramica) (Fig. 4) (Berruto et al. 2014). Each layer is characterized by a defined proportion between hydroxyapatite (HA) and de-antigenated equine collagen 1, thus imitating either subchondral bone, tidemark or cartilage surrounding the recipient site (Kon et al. 2010).

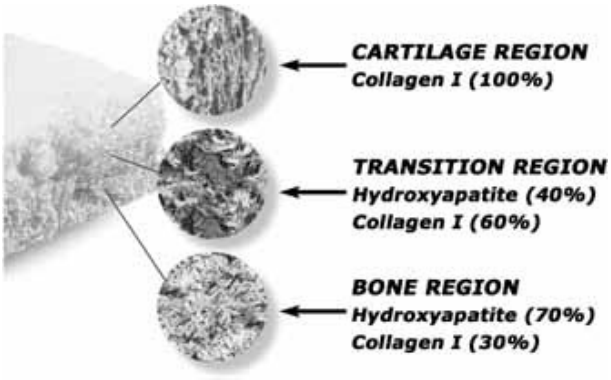

Figure 4: The three layers of the MaioRegen® scaffold and their composition are shown at a macroscopic and a molecular level (Kon et al. 2010).

The cartilaginous layer, consisting of Type I collagen (100 %), has a smooth surface to guarantee low friction during joint movement. The intermediate layer (tide mark-like) consists of a combination of Type I collagen (60 %) and HA (40 %), whereas the lower layer consists of a mineralized blend of Type I collagen (30 %) and HA (70 %) reproducing the sub-chondral bone layer. Each layer is separately synthesized by a standardized process starting from an atelocollagen (a non-immunogenic collagen, isolated from equine tendon) aqueous solution (1% w/w) in acetic acid. The upper, non-mineralized chondral layer only consists of type I collagen (Opocrin S.p.A., Modena, Italy), the intermediate and the lower layers are obtained by nucleating bone-

like, nanostructured, non-stoichiometric HA into self-assembling collagen fibers, similar to the process during biological neo-ossification. The final construct is obtained by physically combining the layers on top of a Mylar sheet under freeze-drying and gamma-sterilization at 25 kGy (Kon et al. 2009).

There are currently no data describing the specific behavior of this product in a detailed experimental in vitro model, but several studies have used this product either in experimental in vivo studies or in the clinical setting (Delcogliano et al. 2014, Filardo et al. 2013, Kon et al. 2010). The failure of the top layer of this product to fully reproduce the principal anatomical features of hyaline cartilage tissue is a known bio-technical limitation (Brix et al. 2016).

3 OBJECTIVES OF THE STUDY

The objectives of this study were to analyze the behavior of the osteochondral implant system MaioRegen® for the first time in an in vitro model and use the results as a basis for future preclinical and clinical studies assessing its suitability for the therapy of osteochondral defects (Berruto et al. 2014).

The following working hypotheses were tested:

1. The experimental in vitro model is suitable for multimodal and high-throughput pre-testing of implants intended for the clinical regeneration of osteochondral defects
2. The OAT group is a suitable and representative control group by mimicking the clinically established treatment concept of osteochondral autologous transplantation
3. MaioRegen® supports the regeneration of the osteochondral defect (incl. cell migration and tissue formation) in the in vitro model by its three-layered physicochemical and molecular structure
4. The combination of histology, RT-PCR, biochemistry, and biomechanical testing is sufficient to address the behavior of the 'host' osteochondral cylinder and the implant, as well as potential reciprocal cross-talk.

For this purpose, a novel osteochondral implant model was developed based on osteochondral cylinders resected from bovine femoral condyles using standardized punches. The cylinders were then filled with either the OAT implant or the MaioRegen® scaffold and cultured for periods of up to 10 weeks.

After 0, 4, 8 and 10 weeks, samples were subjected to (immuno-) histological examinations (HE, Safranin-O; aggrecan staining) and biomechanical testing. In addition, they were analyzed at a transcriptional (gene expression of collagen 1, collagen 2, aggrecan, and COMP) and protein level (DAB- test for tissue proteoglycan analysis; ELISA for collagen 1, collagen 2, and aggrecan in supernatants; Fig. 5).

The major advantages of the novel model are: a) it mimicks the in situ interactions of the recipient site and osteochondral implants; b) it allows to separately investigate each tissue component of the recipient cylinder and the implant; c) it permits to explore local cross-talk between the corresponding tissue type of recipient cylinder and implant.

Work-flow

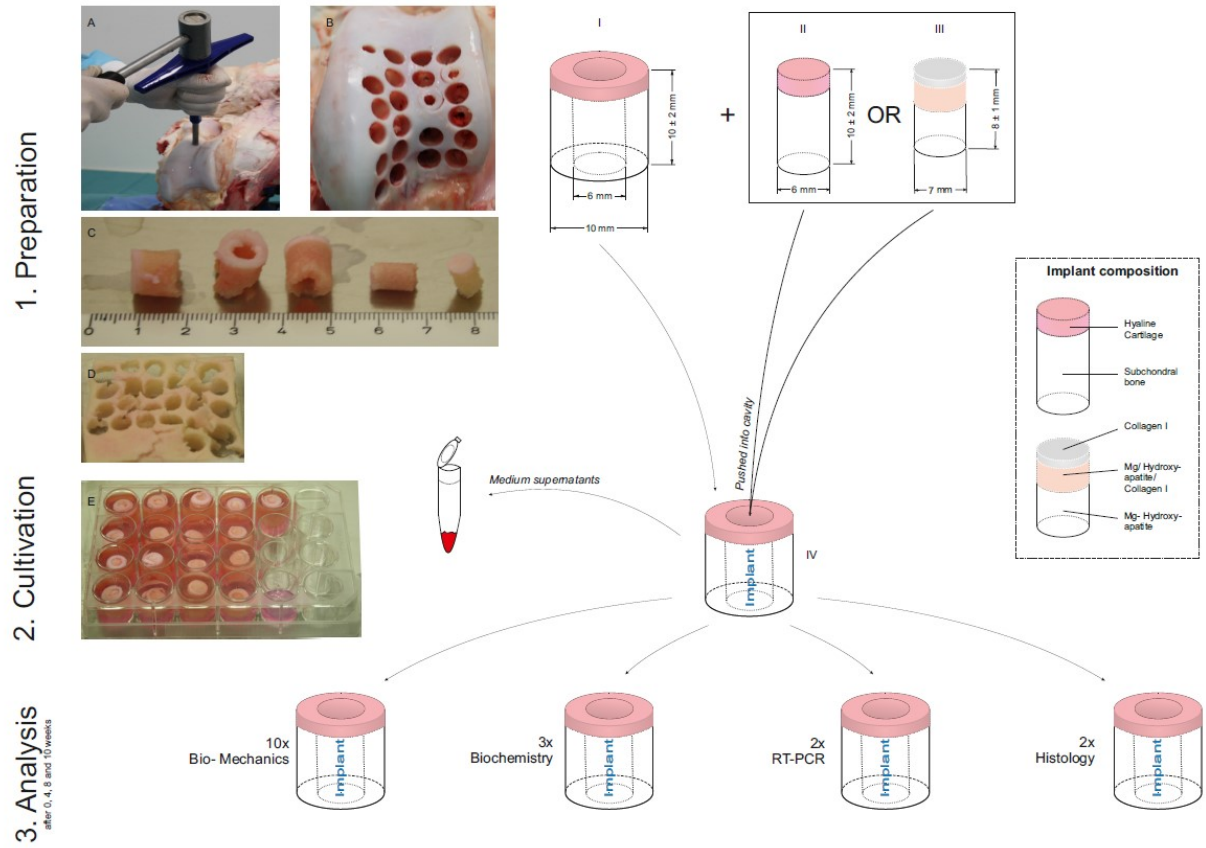

Figure 5: Principal workflow for the preparation, cultivation and analysis of the in-vitro model for the investigation of either MaioRegen® scaffolds or OAT cylinders. I= osteochondral cylinder, II= autologous osteochondral implant/ transplant (OAT), III= MaioRegen® scaffold

4 MATERIALS AND METHODS

4.1 Materials

4.1.1 Chemicals, solutions, and cell culture medium

Name	Company
Acetone	Carl Roth GmbH + Co. KG, Karlsruhe, Germany
Agarose-Gel	Invitrogen™, Carlsbad,CA, USA
Aquatex™	Merck KGaA, Darmstadt, Germany
β – Mercaptoethanol	Sigma-Aldrich™, St. Louis, MO, USA
Basic solution	Heraeus Kulzer GmbH, Hanau, Germany, Technovit 9100®
Chondroitinase ABC from Proteus	Sigma-Aldrich™, St. Louis, MO, USA
Dako Proteinase K	Dako™-Agilent technologies, Hamburg, Germany
3,3' Diaminobenzidine tablets	Sigma-Aldrich™, St. Louis, MO, USA
1,9- Dimethyl-Methylene Blue zinc chloride double salt	Sigma-Aldrich™, St. Louis, MO, USA
Dimethybenzol	Carl Roth GmbH + Co. KG, Karlsruhe, Xylene- Isomere
Cell-Culture Medium solution	gibco® by life technologies™, Darmstadt, Germany, DMEM/F-12 (1:1) (1X) + GlutaMAX™ -I
EDTA dinatriumsalz dihydrat	Carl Roth GmbH + Co. KG, Karlsruhe
Eosin	Hollborn & Söhne GmbH & Co. KG, Leipzig, Germany
Ethanol > 99.5%	Carl Roth GmbH + Co. KG, Karlsruhe
Fast Red TR/ Naphtol AS-MX	Sigma-Aldrich™, St. Louis, MO, USA
FBS- Fetal Bovine Serum	Lonza™, Basel, Switzerland, FBS- BioWhittaker®
Gentamicin	gibco® by life technologies™, Darmstadt, Germany
Glycine	Carl Roth GmbH + Co. KG, Karlsruhe, Germany
Goat serum	Dako™-Agilent technologies, Hamburg, Germany
Guanidium chloride	Merck KGaA, Darmstadt, Germany
Guanidinium-thiocyanate	Life technologies™, Carlsbad,CA, USA, TRIzol®
Hardener One	Heraeus Kulzer GmbH, Hanau, Germany, Technovit 9100®
Hardener Two	Heraeus Kulzer GmbH, Hanau, Germany, Technovit 9100®
Hematoxyline	Hollborn & Söhne GmbH & Co. KG, Leipzig, Germany
Hydrochloric acid	Carl Roth GmbH + Co. KG, Karlsruhe, Germany, fuming 37 %
iQ™ SYBR® Green Supermix	Bio Rad Laboratories, Inc., Hercules, CA, USA
Isotype Antibody	Sigma-Aldrich™, St. Louis, MO, USA, (goat anti mouse IgG)
Isotype Antibody	Dako™-Agilent technologies, Hamburg, Germany, (rabbit IgG)
Insulin, Transferrin, Selen (ITS)	Lonza™, Basel, Switzerland, FBS- BioWhittaker®
K-Mount powder/ solution	Not applicable
Light green-solution	Hollborn & Söhne GmbH & Co. KG, Leipzig, Germany
Osteodec	Labolan®, Navarra, Spain
PMMA-powder	Heraeus Kulzer GmbH, Hanau, Germany, Technovit 9100®
Primary anti-aggrecan antibody	Sigma-Aldrich™, St. Louis, MO, USA, (rabbit anti Aggrecan)

Primary anti-collagen 1 antibody	Sigma-Aldrich™, St. Louis, MO, USA, (rabbit anti Collagen I)
Primary anti-collagen 2 antibody	Acris Antibodies, Inc., San Diego, CA, USA, (BP8008 α type II Collagen)
Proteinase K - concentrate	Dako™- Agilent technologies, Hamburg, Germany
Regulator	Heraeus Kulzer GmbH, Hanau, Germany, Technovit 9100®
Cell buffer	Qiagen™, Venlo, Netherlands, RLT-Buffer
RNA extraction kit	Qiagen™, Venlo, Netherlands, RNeasy® Mini Kit
Phenol/Chloroform	Carl Roth GmbH + Co. KG, Karlsruhe, Germany, Roti®-Phenol/Chloroform
Safranin- O solution	Hollborn & Söhne GmbH & Co. KG, Leipzig, Germany
Secondary antibody Aggrecan	Dako™-Agilent technologies, Hamburg, Germany, (goat anti rabbit)
Secondary antibody Collagen I /II	Dako™-Agilent technologies, Hamburg, Germany, (goat anti rabbit)
Sodium chloride	Merck KGaA, Darmstadt, Germany
RNA amplification kit	Invitrogen™, Carlsbad,CA, USA, SuperScript® RNA Amplification Kit
Trisaminomethane hydrochloride	Sigma-Aldrich™, St. Louis, MO, USA, TRIS-buffer
Hydrogen Peroxide	Sigma-Aldrich™, St. Louis, MO, USA, H_2O_2, 3%

Table I: Chemicals, solutions and cell culture medium

4.1.2 Instruments

Name	Company/ *Product*	Other specifications
Microscope with camera	Carl Zeiss AG, Oberkochen, Germany, *AxioCam HRc*	
Microscope	Carl Zeiss AG, Oberkochen, Germany, *Axiophot Microscope*	
Centrifuge	Eppendorf AG, Hamburg, Germany, *Centrifuge 5415 D*	
Centrifuge	Eppendorf AG, Hamburg, Germany, *Centrifuge 5810 R*	
Desiccator	ThermoScientific®, Waltham, MA, USA, *Nalgene™ Classic Desiccator*	
Digital Slide Scanner	*Hamamatsu®,* NanoZoomer-XR Digital slide scanner C12000, , Japan	
Freezer	Cryo Freezer (-80°C)	set at -80°C
Microplate reader	BMG Labtech GmbH, Ortenberg, Germany, *FLUOStar Optima*	
Freezer	Cryo Freezer (-20°C)	Set at -20°C
Incubator	Heraeus, Kleinostheim, Germany*, Hera cell®_1 - incubator*	Temp.:36.5°C, 5.0% CO_2
Incubator	Memmert, Schwabach, Germany, *CO_2 incubator INCOmed*	
Magnetic stirrer	Heidolph Instruments GmbH & Co.KG, Schwabach, Germany, *MR3001*	

Microtome	Microm, Walldorf, Germany, *HM 355-Micromtome*	
Cell culture bench	Clean Air™, Sanford, Maine, USA	
Cycler	Bio Rad Laboratories, Inc., Hercules, CA, USA, *Mastercycler iCycleriQ®*	
Pipette	Brand GmbH & Co. KG, Wertheim, Germany, *Accu-jet*	
Multi-channel pipettes	Eppendorf AG, Hamburg, Germany	Variable Volumes: 1-10 µl, 100-1000 µl
Microdismembrator	Braun, Melsungen, Germany	
pH Meter	Mettler- Toledo, Columbus, Switzerland, *pH Meter MP 220*	
Refrigerator	Siemens AG, Düsseldorf, Germany	set at 7°C
Sterile set of instruments (scalpel, forceps)	Schubert & Weiss GmbH, Munich, Germany	
Single channel pipettes	Eppendorf AG, Hamburg, Germany	Variable Volumes: 2-20 µl, 10-100 µl, 20-200 µl, 100-1000 µl
Spectrophotometer	Peqlab, Biotechnologie GmbH, Erlangen, Germany, *Spectrophotometer Nano Drop® ND- 1000*	
Thermomixer	Eppendorf AG, Hamburg, Germany, *Thermomixer (comfort)*	1.5 ml and 2.0 ml
Shaker	Scientific Industries Inc., New York, USA, *Vortex Genie 2*	120 V, 60 Hz
Scale	Sartorius, Göttingen, Germany, *Weight scale BP 211 D*	
Universal testing machine	Fa. Zwick, Ulm, Germany, *Zwicki 1120*	

Table II: Instruments

4.1.3 Consumables

Name	Company/*Product*
ELISA Detection Kit	Blue Gene,
Bone Graft Harvester	Arthrex™ Med. Inst. GmbH, Karlsfeld
Bone Graft Harvester	Arthrex™ Med. Inst. GmbH, Karlsfeld
Bovine knee joints	Fleischerei Zitzmann, Erfurt, Germany AND Schlachthof Weibersheim
Tubes	BD Biosciences, Heidelberg, Germany, *Falcon® tubes*
Scaffold	Finceramica, Faenza, Italy, *MaioRegen®*
Suspension-Culture-Plate	Greiner bio-one*CELLSTAR®*
Parafilm “M”	BEMIS
Petri-dish	BD Biosciences, Heidelberg, Germany, *BD Falcon™*
Pipette filtered tips	Eppendorf AG, Hamburg, Germany, *Filtertips*
Pipette tips	Greiner Bio –One GmbH, Frickenhausen, Germany, *Sterile tips CellStar™*
Microscope slides	Gerhard Menzel GmbH, Braunschweig
ELISA Detection Kit	Chondrex, Inc. Redmond, WA, USA

Table III: Consumables

4.1.4 Software

Name	Company	Version
AxioVision	Carl Zeiss Microscopy GmbH, Oberkochen, Germany	4.8.3. SP1
Excel®	Microsoft Inc., Redmond, WA, USA	Microsoft Office 2010
iCycler iQ™	Bio Rad Laboratories, Inc., Hercules, CA, USA	3.1
MARS Data Analysis Software	BMG Labtech GmbH, Ortenberg, Germany	2.40
NDP-Viewer	Hamamatsu®, Japan	2.0
Optima	BMG Labtech GmbH, Ortenberg, Germany	2.20R2
SPSS	SPSS, Chicago, USA	Win Version 22.0

Table IV: Software

4.2 Methods

4.2.1 Preparation of bovine osteochondral cylinders and cell culture

Bovine knee joints (German Holstein Friesian Cattle) were obtained on the day of slaughter. Osteochondral cylinders were aseptically prepared by punching out a central cylinder with a diameter of 6 mm and a length of 10 ± 0.2 mm using a 6 mm Bone Graft Harvester – Recipient punch system (Arthrex™).

Another osteochondral punch with a diameter of 10 mm and a length of 10 ± 0.2 mm was then centered on the initial 6 mm punch, assuring a circular wall width of 2 mm (Fig. 5). After lifting the osteochondral rings off the underlying bone, they were stored in freshly prepared cell culture medium (gibco® by life technologies™; for composition see below).

The scaffolds (MaioRegen®, Finceramica™) were first moistened with cell culture medium, then cut to a diameter of 6 mm using the appropriate donor punch (Arthrex™) and finally press-fit inserted into the osteochondral rings. As a control group, the previously harvested central cylinders were reimplanted into the osteochondral rings of their origin in analogy to the procedure during osteochondral autologous transplantation and subsequently cultured as the scaffold group.

Seventeen wells of a 24-well plate were then evenly filled with a total of 9 ml of hot 2% agarose (Invitrogen™). Before complete hardening of the gel, central cavities with a diameter of 10 mm were generated in the gel with a manufactured stamp (Fig. 6). The osteochondral rings were then embedded into the agarose cavities in an upright fashion, with the cartilage facing the top. This guaranteed a sufficient nutrition via diffusion and a stable footing against the shear forces during medium exchange.

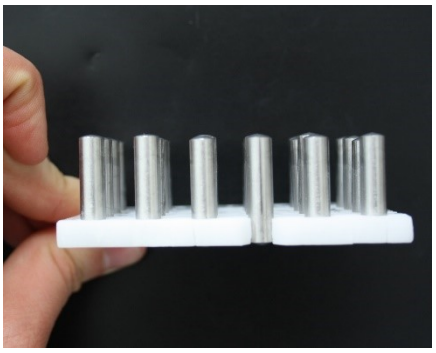

Figure 6: Cavities with a diameter of 10 mm were generated in the hot liquid agarose gel using this stamp.

For each time point (4, 8 and 10 weeks) and each group (scaffold and OAT), an extra plate was prepared. The well plates were then covered and stored in an incubator (Heraeus®) at 37.5°C, 5% CO_2 for 48 h with a cell culture medium exchange every second day. The supernatant of the wells was collected every other day, frozen and eventually used for analysis.

Cell culture medium (500 ml Cell-Culture Medium DMEM/F-12(1:1) + GlutaMAX™ (gibco® by life technologies™), 25 ml FBS Bio- Whittaker® (Lonza™), 5 ml Gentamicin (gibco® by life technologies™) and 500 µl ITS (Lonza™)) was freshly prepared before initiating a new test series and before each medium exchange.

4.2.2 Histology and immunohistochemistry

Fresh, non-cultured (0 weeks), and cultured (4, 8, 10 weeks) implant-containing osteochondral rings were harvested and stored in 100 % acetone at -7°C for a period of at least 72 h.

For further preparation, samples were transferred to fresh acetone (Carl Roth GmbH + Co. KG) for one hour, before washing them twice in Xylene (Carl Roth GmbH + Co. KG) for an hour each. They were then incubated in a 1:1 acetone and basic solution (Heraeus Kulzer GmbH) mixture for 20 min.

Samples were then immersed in basic solution and Hardener One (Heraeus Kulzer GmbH, concentration of 0.01 g/ml) for one hour before being rinsed with infiltration solution (Heraeus Kulzer GmbH, 25 ml Basic solution destabilized with Aluminum Oxide, 2 g PMMA powder (Heraeus Kulzer GmbH) and 0.1 g Hardener One). Thereafter, the samples were stored in a desiccator for 7 days.

For embedding of the samples, two solutions A and B were prepared. Solution A was composed of 25 ml Basic solution, 4 g PMMA powder and 0.15 g Hardener One; solution B contained only 2.2 ml Basic solution, 0.2 ml Hardener Two and 0.1 ml of

Regulator solution. Solutions A and B were mixed in a 9:1 ratio and used to fix the osteochondral cylinders. After 48 h of hermetically sealed storage at -7°C, the blocks were fixed in a mounting ring using K-Mount powder and solution.

Blocks were then sectioned on a microtome and subsequently either fixed on Polysine or on Superfrost slides (Gerhard Menzel GmbH).

Before staining, the histological sections were de-plastinated by incubating the sections at 37°C for 30 min and washing in Xylene for 2 x 20 min and M- acetate for 20 min (Carl Roth GmbH + Co. KG). Sections were then washed with 96% alcohol for 2 x 2 min (Carl Roth GmbH + Co. KG) and with 70% alcohol for 2 x 2 min. The samples were then rinsed with distillated water.

Finally, the stained histological sections were evaluated using semi-quantitative scores. The cartilaginous parts were rated according to a modified O'Driscoll score. For the other parts, this scoring system was adapted in a reasonable manner. Due to the use of a score (that was actually designed to evaluate cartilage) in bone tissue, an increase in the score may implicate a differentiation in cartilage but a de-differentiation in bone (O'Driscoll et al. 1986). In addition, other features such as the lateral bonding and cell migration were analyzed. For a better comprehension, scores for structural and regenerative features were summarized separately (Table 1 and 2).

Tissue	HE	Safranin-O	Aggrecan
Cartilage Ring	0 = intact lamina splendens 1= loss of lamina splendens 2= moderate cartilage erosion 3= massive loss and destruction of cartilage.	0= intact proteoglycan (PG) structure 1= slight PG loss 2= moderate PG loss 3= massive PG loss	0= large aggrecan depositions 1= slight aggrecan loss 2= moderate aggrecan loss 3= massive
Bone Ring	0= intact lamellar bone 1= slightly decreased bone density (single foci) 2= decreased bone density (several foci) 3 = osteoporotic, (necrotic) bone tissue	not applicable	not applicable
Implant cartilaginous part	0= intact implant 1= slightly dissolving implant/tissue 2= massive dissolution of implant 3= complete loss of implant	0= intact proteoglycan (PG) structure 1= slight PG loss 2= moderate PG loss 3= massive PG loss ONLY FOR OAT GROUP	0= large aggrecan depositions 1= slight aggrecan loss 2= moderate aggrecan loss 3= massive ONLY FOR OAT GROUP
Implant osseous part	0= intact implant 1= slightly dissolving implant/tissue 2= massive dissolution of implant 3= complete loss of implant	not applicable	not applicable

Table 1: Scoring system for the structural/ histological evaluation of the histological sections.

Tissue	HE	Safranin-O	Aggrecan
Cartilage Ring	0= no lateral bonding 1= partial bonding 2= strong bonding 3= complete tissue integration	not applicable	not applicable
Bone Ring	0= no lateral bonding 1= partial bonding 2= strong bonding 3= complete tissue integration	0= no PG 1= single PG structures 2= connected PG structures 3= large, dominating PG structures	0 = no signal 1= insular foci 2= numerous foci 3= large deposits
Implant cartilaginous part	0= no cells migrated 1= single cells migrated 2= numerous cells migrated 3= complete layer/ organized network of migrated cells.	0= no PG 1= single PG structures 2= connected PG structures 3= large, dominating PG structures ONLY FOR MAIOREGEN	0 = no signal 1= insular foci 2= numerous foci 3= large deposits ONLY FOR MAIOREGEN
Implant osseous part	0= no cells migrated 1= single cells migrated 2= numerous cells migrated 3= complete layer/ organized network of migrated cells.	0= no PG 1= single PG structures 2= greater, connected PG structures 3= large, dominating PG structures	0 = no signal 1= insular foci 2= numerous foci 3= large deposits

Table 2: Scoring system for the histological evaluation with focus on regenerative features.

4.2.2.1. Hematoxyline Eosin (HE) - Staining

De-plastinated sections were washed in distillated water for 30 min and then dipped into Hematoxylin (Hollborn & Söhne GmbH & Co. KG) for 20 s before washing them in water (aqua nondest) for 10 min. After this step, the sections were incubated in Eosin (Hollborn & Söhne GmbH & Co. KG) for 10 s and rinsed again with water. Thereafter, sections were passed through ascending concentrations of alcohol ending in xylene (starting with Isopropanol (2-propanol) twice for 2 minutes, followed by 96% ethanol for 2 minutes and xylene twice for 5 min. Finally, the stained sections were covered or embedded with mounting media (Aquatex®, Merck AG).

4.2.2.2. Safranin-O Staining

De-plastinated sections were stained in Safranin- O solution (Hollborn & Söhne GmbH & Co. KG) for 4 min, washed in distilled water and then incubated in Light-Green (Hollborn & Söhne GmbH & Co. KG) for another 4 min before passing them through the same ascending alcohol concentrations as above.

4.2.2.3. Immunohistological staining

For aggrecan staining, histological sections were enzymatically digested by Chondroitinase ABC (Sigma- Aldrich™) 1:40 in 0.1 M Tris-HCl for 90 min at 37°C before decalcifying them in Osteodec (Labolan®) at 37°C for 1 h. After this and all

following steps, sections were washed in TBS buffer solution (pH =7.4). Thereafter, the endogenous peroxidase was blocked with 3% H_2O_2 (Sigma- Aldrich™) and nonspecific binding sites were blocked by 10% goat serum (Sigma- Aldrich™). Aggrecan was detected by Aggrecan Primary Antibodies 1:50 in TBS (Sigma-Aldrich™). Subsequently the sections were incubated over night at 4°C with Iso-goat-anti-mouse IgGs 1:1000 in TBS (Dako™- Agilent technologies).

The following day, the sections were incubated with amplifying, secondary antibodies of the aggrecan system (Dako™- Agilent technologies; dilution 1:30 in TBS) and then stained with Fast Red for aggrecan (Sigma- Aldrich™). The sections were then counterstained with hematoxylin, washed in tap water, and covered with Aquatex (Merck KG).

4.2.3 RNA isolation

Osteochondral samples containing implants were dissected into cartilage ring, implant top (either the upper, collagen-enriched layer of the MaioRegen scaffold implant or the cartilaginous part of the OAT implant), bone ring and implant bottom (either the lower, hydroxylapatite-containing layers of the scaffold or the osseous part of the OAT implant) as shown in Fig. 4 and 5. The samples were then separately vortexed for one minute in lysis- buffer consisting of 4950 µl RLT- buffer (Qiagen™) and 50 µl β–Mercaptoethanol (Sigma- Aldrich™). Implant top and bottom were then shock frozen in liquid nitrogen, whereas cartilage rings and bone rings were separated from the lysis-buffer first before shock freezing each, tissue and buffer.

Cartilage rings, bone rings, implant top and bottom were transferred into Trizol® (Life technologies™), mechanically broken up using scissors or a microdismembrator (Braun®). There bone tissue was milled for 1 min with an agitated grinding ball in a nitrogen-cooled, stainless steel container at a frequency of 33 Hz and an amplitude of 18 mm. Thereafter, the samples were centrifuged at 12 x 10^3 rpm for 3 min before transferring the supernatants into 180 µl of phenol chloroform (Carl Roth GmbH + Co. KG). There probes were then incubated for another 3 min before centrifuging at 12 x 10^3 rpm with a Centrifuge 5415 D (Eppendorf AG) for 10 min. The upper layer of the resulting tri-layered solution was then transferred to 300 µl of 80% ethanol. The RNA isolated from the lysis-buffer-solutions of the cartilage and bone rings were directly used for subsequent RNA isolation.

The following procedure of RNA isolation was performed using an RNA extraction kit in accordance with the instructions of the supplier (Qiagen™). In detail, the RNA

containing ethanol solution was transferred onto an RNeasy column® and subsequently centrifuged at 1 x 10^4 G for 1 min. The throughput was discarded and the column rinsed with 500 µl of RW1® buffer solution. The columns were then again centrifuged at 1 x 10^4 G for 1 min. A total of 70 µl of RDD buffer® and 10µl of DNase 1® were added to the column, which was then incubated for 15 min. The column was then washed with 500 µl of RW1 buffer® and centrifuged 1 x 10^4 G for 30 s. This step was repeated three times. Then the column was centrifuged at 1.2 x 10^4 G for 2 min, transferred into a new Eppendorf® tube, and rinsed with 15 µl RNase-free water. RNA was eluted by centrifugation at 1 x10^4 G for 1 min.

Finally, the concentration of the purified RNA was measured using the NanoDrop ND-1000 (Peqlab, Biotechnologie GmbH).

4.2.4 Reverse transcription and quantitative PCR

Total RNA eluate (15 µl) was primed with oligo(d)T (Invitrogen™) and reverse-transcribed for one hour at 42°C using SuperScript-II reverse transcriptase (Invitrogen™).

qPCR reactions were carried out as previously described with cloned standards for the quantitation of bovine collagen 1, collagen 2, aggrecan, COMP and the housekeeping gene bovine Aldolase. qPCR was then performed on a Mastercycler iCycleriQ® (Bio Rad Laboratories, Inc.) with the primer pairs and PCR conditions presented in Table 3.

For the evaluation collagen 2/1 and aggrecan/collagen 1 ratios were calculated. In cartilaginous tissues, scores larger than 1 indicate differentiating processes; in osseous tissues, however, scores smaller than 1 indicate differentiating processes.

Gene	Primer 5' -> 3'	Primer 3' -> 5'	Product length in bp	T annealing in °C	Melting T product in °C
Aldolase	CGC CCC CGA TGC AGG GAT TC	CAC CGG ATT GTG GCT CCG GG	314	58	88
COMP	ATG CGG ACA AGG TGG TAG AC	TCT CCA TAC CCT GGT TGA GC	498	58	94
Aggrecan	CAG AGT TCA GTG GGA CAG CA	AGA CACA CCA GCT CTC CTG AA	189	60	84
Collagen I	ACA CAG GTC TCA CCG GTT TC	AGC CAG CAG ATC GAG AAC AT	185	60	86
Collagen II	CAT CTG GTT TGG AGA AAc CAT C	GCC CAG TTC AGG TCT CTT AG	600	61	83

Table 3: General amplification protocol (45 cycles): initial denaturation for 2 min at 96°C, specific primer annealing temperature as stated above for 20 s, amplification at 68°C for 15 s, additional heating to 5°C below the melting temperature of the PCR product as above. General melting curve protocol (one cycle): denaturation for 1 s at 95°C; cooling to 5 °C above the primer annealing temperature (holding temperature for 10 s); heating to 95°C (0.1°C/s); final cooling over 8 min to 40°C.

The relative concentrations of cDNA present in the samples were calculated using the standard curves. For the normalization of the cDNA concentration in each sample and the comparability of the calculated mRNA expression in the analyzed samples, the housekeeping gene aldolase was also amplified. Product specificity was confirmed by melting curve analysis and initial cycle sequencing of the PCR products.

4.2.5 Enzyme-linked immunosorbent assay (ELISA)

The medium supernatants of the culture medium exchange of weeks 0, 4, 8 and 10 were analyzed by pooling supernatants of the same week and group.

Collagen 1, collagen 2 and aggrecan concentrations in the supernatants of the culture medium were measured according to the protocols of commercially available ELISA-Kits (Chondrex™, BlueGene).

Absorption was measured using a Fluostar Optima™ Reader (BMG Labtech GmbH) at 490 nm.

4.2.6 Quantification of glycosaminoglycans

For the quantification of sulphated glycosaminoglycans, the dimethylene blue binding assay (DMB) was used (Chandrasekhar et al. 1987). Samples were mechanically broken up into their subparts (cartilage ring, implant top, bone ring and implant bottom), incubated in 1 ml guanidium hydrochloride (Merck KGaA) at 4 °C for 48 h, centrifuged at 12 x 10^3 rpm for 1 h (centrifuge 5810 R, Eppendorf AG), and finally eluted in 700 µl H_2O each.

For the supernatants of the cartilage and bone lysis-buffer the quadruplicated volume of Acetone (Carl Roth GmbH + Co. KG) was added and incubated for 30 min at -20 °C before centrifugation at 12 x 10^3 rpm for 10 min (Centrifuge 5810 R Eppendorf AG). The remaining pellet was then washed in 500 µl Ethanol (70%) and again centrifuged for 5 min at 12 x 10^3 rpm. Supernatants were discarded and the pellet resuspended in 100 µl distilled H_2O.

For the DMB assay, 16 mg 1,9 Dimethylene Blue (Sigma- Aldrich™) were dissolved in 5 ml Ethanol (100%) and 2.37 g NaCl (Merck KG) and 3.04 g Glycine were added (Carl Roth GmbH + Co. KG). The resulting solution was diluted in distilled H_2O to a total volume of 1 l (pH 3).
Absorption was measured using a Fluostar Optima™ Reader (BMG Labtech GmbH) at 525 nm, taking a descending dilution series of bovine nasal septum as a standard.

4.2.7 Biomechanical analysis

Biomechanical testing of samples from the different time points and test series (10 samples each) was performed using a static universal testing machine Zwicki 1120® at the Department of Biomechanics, Technische Universität München. The osteochondral cylinder was fixed and the force necessary to push out the implant from the osseous side with a stamp (5 mm diameter) was measured. Thereafter, the stamp was passed through the empty cylinder without an implant. This value ($F_{max(empty)}$) was subtracted from the value of the ring still containing an implant ($F_{max(insert)}$). Therefore, the adjusted value for the biomechanical load bearing capacity of the implant was $\Delta F = F_{max(insert)} - F_{max(empty)}$.

4.2.8 Statistics

All the data were entered into an Excel database (MS Office Excel 2007, Microsoft, Redmond, Washington). Statistical analysis was performed using a nonparametric Friedman test to detect differences among multiple test groups and, subsequently, using a nonparametric Wilcoxon-Mann-Whitney test for the comparison of individual groups. P values ≤ 0.05 were considered statistically significant.

5 RESULTS

5.1 Histology

5.1.1 Overview of HE, Safranin-O and Aggrecan (immuno-)stainings

t in weeks	OAT	MaioRegen
0	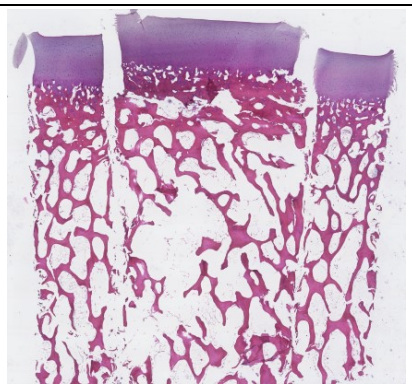	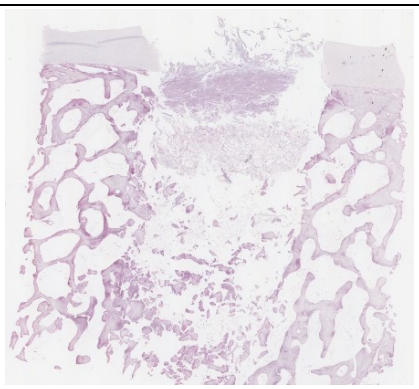
4	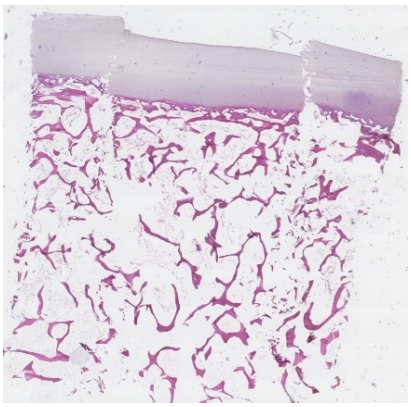	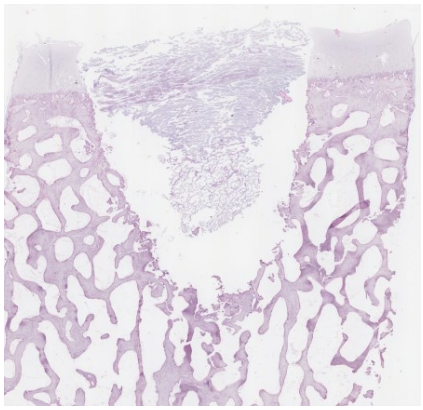
8	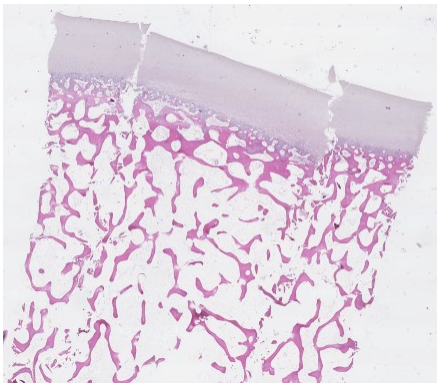	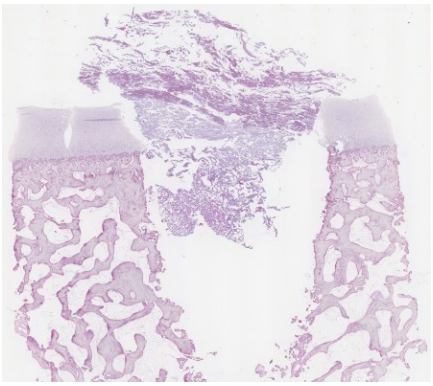
10		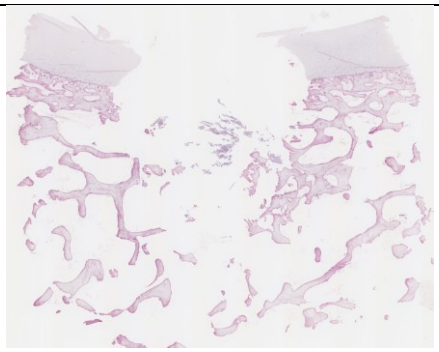

Fig. 7: Overview of OAT and MaioRegen sections at 0, 4, 8, and 10 weeks (**HE-staining**; Magnification 9x).

t in weeks	OAT	MaioRegen
0	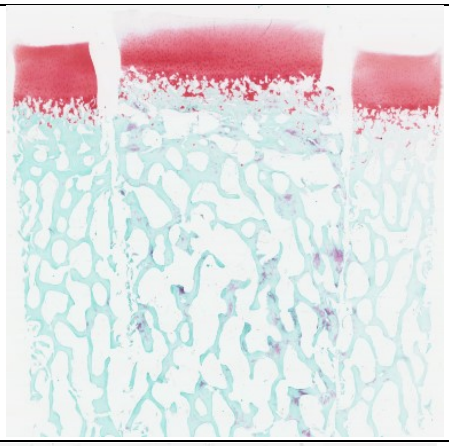	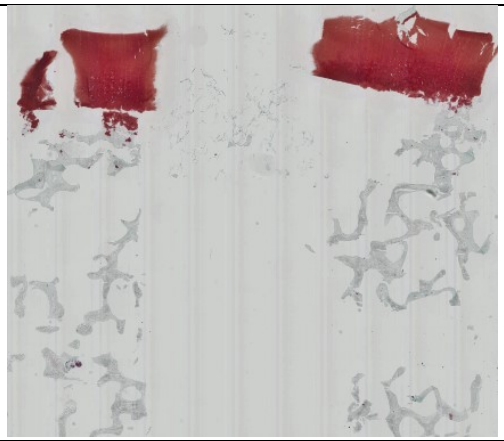
4	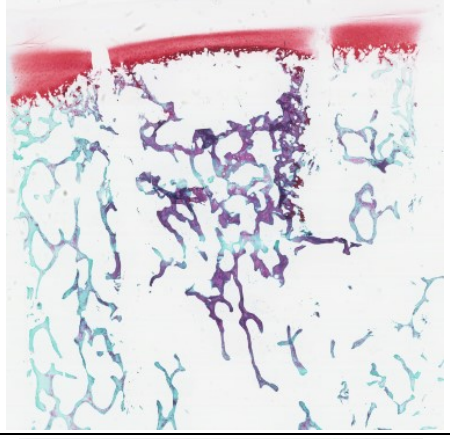	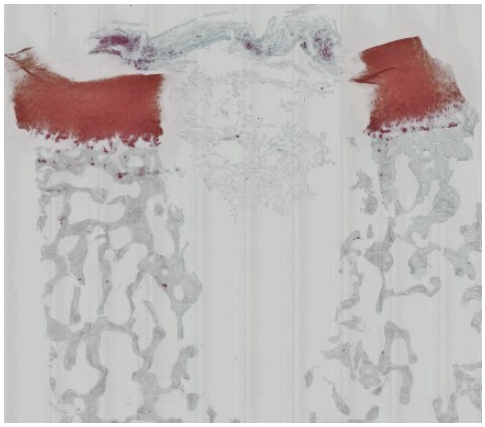
8	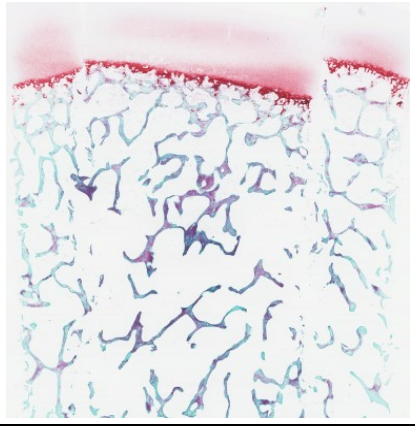	
10		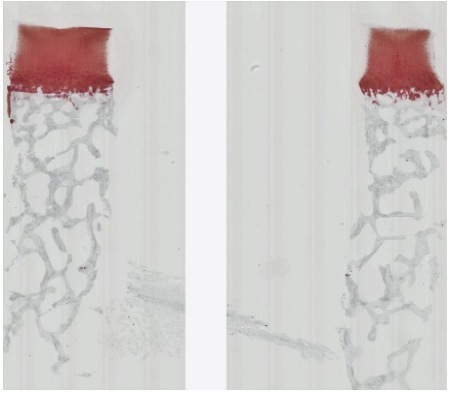

Fig. 8: Overview of OAT and MaioRegen sections at 0, 4, 8, and 10 weeks (**SO-staining**; Magnification 9x).

t in weeks	OAT	MaioRegen
0		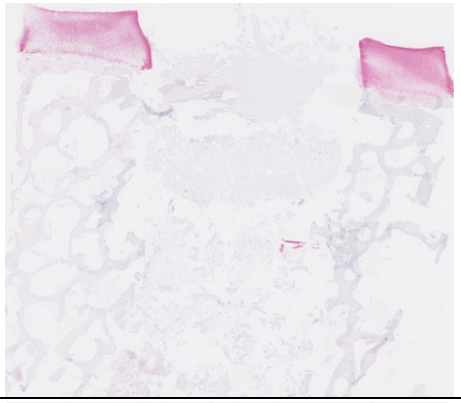
4	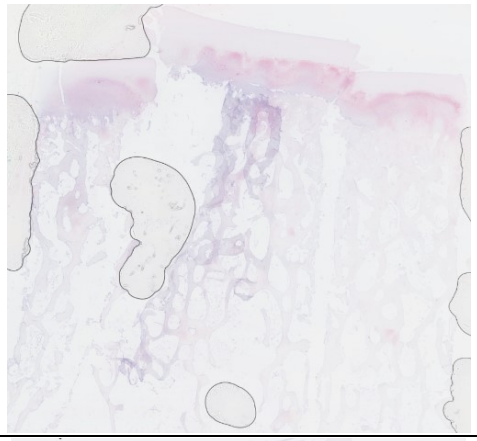	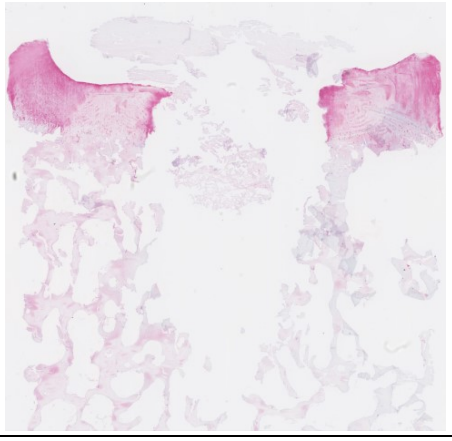
8	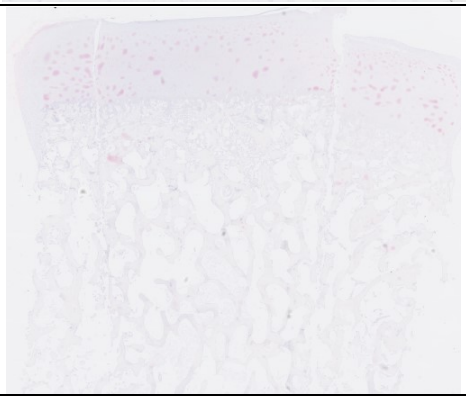	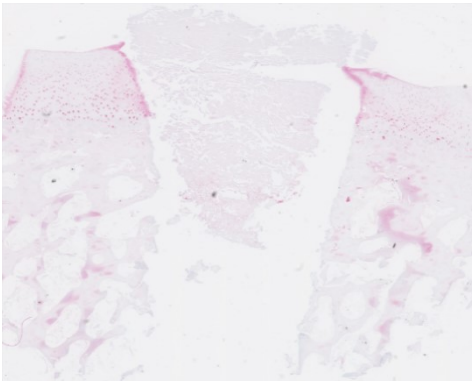
10		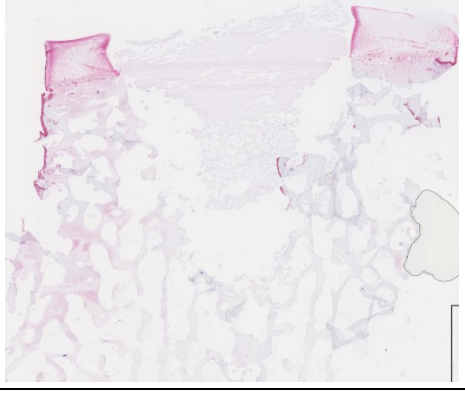

Fig. 9: Overview of OAT and MaioRegen sections at 0, 4, 8, and 10 weeks (**aggrecan immunostaining**; Magnification 9x).

The data for the semiquantitative histological description are provided in Tables 4 and 5 (see below) and are based on semiquantitative scores (see Methods; Tables 1 and 2).

Cartilage ring

HE staining: In both the OAT and the MaioRegen group, the cartilage rings largely maintained their shape (Fig. 7). In addition, no signs of necrosis or tissue degeneration were observed, except for occasional empty chondrocyte lacunae. Those were found especially in the surface and transitional layer. This overall largely maintained tissue integrity was reflected by low tissue degradation scores between 0 and 0.3 in the OAT group and between 0 and 1.1 in the MaioRegen group (Table 4).

In both the OAT and the MaioRegen group, the gap between the cartilage ring and the implants was maintained until 10 weeks of culture and did not show any signs of tissue formation and/or wound healing. Migration of cells onto the cartilage ring was observed in both groups (Abb. 7).

This very limited degree of regeneration was reflected by a low and similar regeneration score for both OAT and MaioRegen (range 0 to 0.6; Table 5).

Safranin-O staining: In the OAT and the MaioRegen group, there was a clear decrease of the staining intensity over time in the cartilage ring, which is indicative for a loss of proteoglycan (Fig. 8). Semiquantitative evaluation confirmed a slight to moderate and comparable loss of proteoglycans in both groups (0 to 1.4 for OAT; 0 to 0.8 for MaioRegen; Table 4).

Aggrecan staining: In agreement with the results of the Safranin-O staining, the aggrecan staining in the OAT group was lost over time and initially large, cohesive aggrecan deposits seemed to be redistributed into smaller, multifocal insulae. At 8 weeks, aggrecan staining was primarily observed in the immediate vicinity of the chondrocytes, possibly indicating active cellular aggrecan synthesis (Fig. 9).

These changes resulted in a progressively increased score for the proteoglycan loss for the OAT group from 0 at 0 weeks to 2.0 at 8 weeks (Table 4).

Similar, but quantitatively smaller changes were also observed in the MaioRegen group (Fig. 9). In contrast to the OAT group, however, intense aggrecan signals were found at the interface between the cartilage ring and the cartilaginous part of the MaioRegen scaffold throughout culture (Fig. 9). Also in the MaioRegen group, the score for the aggrecan loss increased from 0 at 0 weeks to 1.6 at 10 weeks (Table 4).

Bone ring

HE staining: In both the OAT and MaioRegen group, also the bone rings maintained their original structure without signs of necrosis or other bone-degrading processes (Fig. 7). This was reflected by low tissue degradation scores between 0 and 0.3 for the OAT group and 0 and 1.0 for the MaioRegen group (Table 4).

In the OAT group, the gap between the bone ring and the implant was continuously closed within 8 weeks of culture. At this time point, the gap between the osseous parts of the implant model could hardly be recognized any more. In addition, cell migration into the neighboring subchondral regions was observed (Fig. 7).

This almost complete closure of the gap was reflected by a very high lateral bonding/regeneration score (up to 2.6 of max. 3; Table 5).

In the MaioRegen group, in contrast, the gap between bone ring and implant was even enlarged with time, at least partially caused by progressive dissolution of the MaioRegen implant. At the same time, the adjacent bone ring showed clear signs of bone formation, as indicated by a diminished size of the original defect and by a condensed edge region with newly formed bone trabeculae (Fig. 7).

This active process resulted in a lack of lateral bonding to the bone ring (significantly lower than in the case of OAT), but a substantial immigration into the implant (see below; Table 5).

Safranin-O staining:

In contrast to the proteoglycan loss in the cartilage ring, both OAT and MaioRegen showed a transient, moderate increase of the proteoglycan-containing cartilage structures with a peak/plateau at 4 weeks, possibly reflecting an attempt to integrate the implant via enchondral ossification (Fig. 8). This resulted in a proteoglycan deposition score of max. 1.6 for OAT and 1.1 for MaioRegen (Table 5).

Aggrecan staining: In both the OAT and the MaioRegen group, the bone ring showed aggrecan signals after 4, 8, and 10 weeks in the areas corresponding to the enhanced proteoglycan deposition detected by Safranin O staining (Fig. 9). However, this was more pronounced in the case of MaioRegen (max. 2.3 for MaioRegen versus max. 1.6 for OAT; Table 5).

Implant cartilaginous part

HE staining: In analogy to the cartilage ring of the neighboring osteochondral cylinder, the cartilaginous part of the OAT implant almost fully maintained its tissue integrity without any signs of necrosis or tissue degradation (Fig. 7), and thus showed very low tissue degradation scores (between 0 and 0.3; Table 4).

In addition, moderate cell migration onto the surface of the OAT implant was observed, reflected in a score of max. 1.1 (Table 5).

Due to its progressive dissolution over time, the 'tissue' integrity of the cartilaginous part of the MaioRegen group was partially or totally lost at 10 weeks (degeneration score of up to 1.4; Table 4). In parallel, there was hardly any cell migration onto this implant part (max. 0.1; Table 5).

Safranin-O staining: As observed for the neighboring cartilage ring, the cartilaginous parts of the OAT implant showed a limited decrease of the staining intensity over time (Fig. 8; proteoglycan loss of max. 0.3 at 8 weeks; Table 4). Due to the complete absence of proteoglycan in the cartilaginous top of the MaioRegen group, hardly any positive Safranin-O staining was detected at any time point.

Aggrecan staining: For both OAT and MaioRegen, the findings were largely comparable with those of the Safranin-O staining, with a slighty higher proteoglycan loss in the OAT group and a very restricted positive signal for aggrecan in the MaioRegen group (Fig. 9; Tables 4, 5).

Implant osseous part

HE staining: In the OAT group, the osseous part of the implant showed a stable structure without signs of necrosis or tissue degradation and thus a degeneration score of 0 (Fig. 7; Table 4).

In contrast, the osseous part of the MaioRegen implant displayed slight dissolution (Fig. 7; max. score 0.6; Table 4), however less marked then for its cartilaginous counterpart (see Table 4). Cell migration onto both the OAT and MaioRegen implants was moderate and comparable (max. 1.5; Table 5).

Safranin-O staining: The osseous part of both OAT and MaioRegen showed moderate to strong proteoglycan deposition with a peak or plateau at 4 weeks (Fig. 8; (Table 5).

Aggrecan staining: In both the OAT and the MaioRegen group, there was a progressive appearance of positive aggrecan signals with a peak or plateau at 4 or 8 weeks, which

was reflected by progressively increasing scores over time (from 0.3 to 2.1 for OAT and 0 to 2.0 for MaioRegen group; Table 5; Fig. 9).

5.1.2 Results of semiquantitative evaluation

After 0, 4, 8, and 10 weeks of cell culture, three investigators rated the histological sections according to scoring system presented in Tables 1 and 2 (see Methods).

Tissue	t in weeks	HE		Safranin-O		Aggrecan	
		OAT	MaioRegen	OAT	MaioRegen	OAT	MaioRegen
Cartilage rings	0 4 8 10	0 0.3 (± 0.5) 0.2 (± 0.4)	0 (± 0) 1.1 (± 0.3) 0.2 (± 0.4) 0.6 (± 0.7)	0 0.4 (± 0.5) 1.4 (± 0.5)	0 0.7 (±0.6) 0.8 (± 0.3) 0.7 (±0.4)	2.4 (± 0.3) 1.4 (± 0.5) 2.0 (± 0)	1.5 (± 0.5) 1.4 (± 0.5) 1.2 (± 0.4) 1.6 (± 0.5)
Bone rings	0 4 8 10	0 0.3 (± 0.5) 0	0 0 0 1.0 (± 0.7)	not applicable	not applicable	not applicable	not applicable
Implant cartilaginous part	0 4 8 10	0 0.4 (± 0.7) 0	0 1.1 (± 0.8) 1.4 (± 0.5)* 1.4 (± 0.5)	0 0.2 (± 0.3) 0.3 (± 0.4)	not applicable	2.0 (± 0.5) 2.4 (± 0.5) 1.0 (± 0)	not applicable
Implant osseous part	0 4 8 10	0 0 0	0 0.6 (± 0.5) 0.4 (± 0.5) 0.5 (± 0.7)	not applicable	not applicable	not applicable	not applicable

Table 4: Degradation of the involved tissue types and components, i.e., degeneration (HE), proteoglycan loss (Safranin-O staining), and aggrecan loss (Aggrecan staining). The respective scoring systems are shown in Table 1 (see Methods). Generally, low values indicate an intact status. *$p \leq 0.05$ versus OAT.

Tissue	t in weeks	HE		Safranin-O		Aggrecan	
		OAT	MaioRegen	OAT	MaioRegen	OAT	MaioRegen
Cartilage ring	0 4 8 10	0 0.6 (± 0.4) 0.3 (± 0.3)	0 0 0 0	not applicable	not applicable	not applicable	not applicable
Bone ring	0 4 8 10	0 2.2 (± 0.3) 2.6 (± 0.5)	0 0* 0* 0	0.7 (±0.4) 1.6 (± 0.5) 1.6 (± 0.5)	0.5 (± 0.5) 0.8 (± 0.3) 1.1 (± 0.3) 1.1 (± 0.3)	0.4 (± 0.5) 1.6 (± 0.5) 0.6 (±0.4)	0.6 (± 0.5) 2 (± 0.7) 1.8 (± 0.6) 2.3 (± 0.5)
Implant cartilaginous part	0 4 8 10	0 0.7 (± 0.6) 1.1 (± 0.9)	0 0 0* 0.1 (± 0.1)	not applicable	0 0.1 (± 0.3) 0 0	not applicable	0 0.3 (± 0.5) 0.2 (± 0.4) 0.1 (± 0.3)
Implant osseous part	0 4 8 10	0 0.7 (± 0.4) 1.5 (± 0.5)	0 1.4 (±0.5) 1.4 (±0.5) 1.5 (± 0.5)	0.8 (± 0.3) 2.6 (±0.5) 2.7 (±0.4)	0* 2.4 (± 0.5) 1.7 (± 0.4) 1.4 (± 0.5)	0.3 (± 0.5) 2.1 (± 0.6) 0.8 (± 0.4)	0 1.7 (± 0.4) 2.0 (± 0) 1.6 (± 0.5)

Table 5: Regenerative properties of the involved tissue types and components, i.e., lateral bonding (cartilage/bone ring) and cell migration (implant; HE staining), as well as proteoglycan deposition (Safranin-O staining; Aggrecan staining). The respective scoring systems are shown in Table 2 (see Methods). Generally, high values indicate a higher degree of regeneration. *$p \leq 0.05$ versus OAT.

5.2 Quantitative RT-PCR

In order to improve visualization and comprehension of the PCR data, small schemes of the respective parts of the osteochondral cylinder and the implants were inserted.

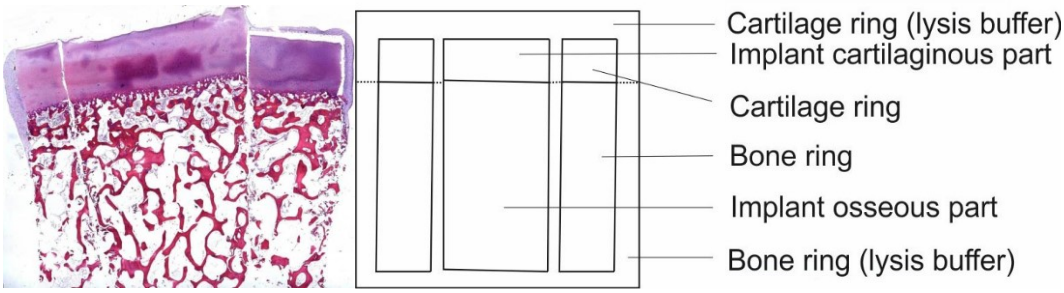

Figure 10: Histological section and simplified scheme specifying the 6 diverse types of tissues/ implant material that were analyzed for gene expression of collagen 1, collagen 2, aggrecan, and COMP.

5.2.1 Cartilage ring

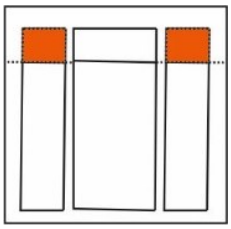

Collagen 1

In the OAT group, collagen 1 mRNA was detected at 4 weeks only, while the MaioRegen group showed a consistently and significantly decreasing mRNA expression from 0 to 10 weeks (Fig. 11).

Collagen 2

Collagen 2 gene expression was approx. 100-fold increased over time in both groups, with a peak at 10 weeks (*p ≤ 0.05 vs. 0 weeks; all time points in the MaioRegen group).

Aggrecan

In the OAT group, gene expression of aggrecan increased up to a peak at 8 weeks and dropped thereafter. In the MaioRegen group, the expression of aggrecan instead continuously decreased to minimal levels at 8 weeks and 10 weeks .

COMP

While there was no COMP expression in the OAT group at any time, decreasing COMP expression was detected in the MaioRegen group at 0 and 8 weeks only.

Collagen 2/1 ratio

Due to the lack of collagen 1 expression at 0, 8, and 10 weeks, the collagen 2/1 ration was not informative for the OAT group. The MaioRegen group showed a consistent, significant increase until 10 weeks, with peak-values more than 2000-fold higher than those at 0 weeks.

Aggrecan/Collagen 1 ratio

As for the collagen 2/1 ratio, the aggrecan/collagen 1 in the OAT group was not informative. In the MaioRegen group, in contrast, this ratio showed 2.5-fold maxima at 4 weeks and 10 weeks (Fig. 11).

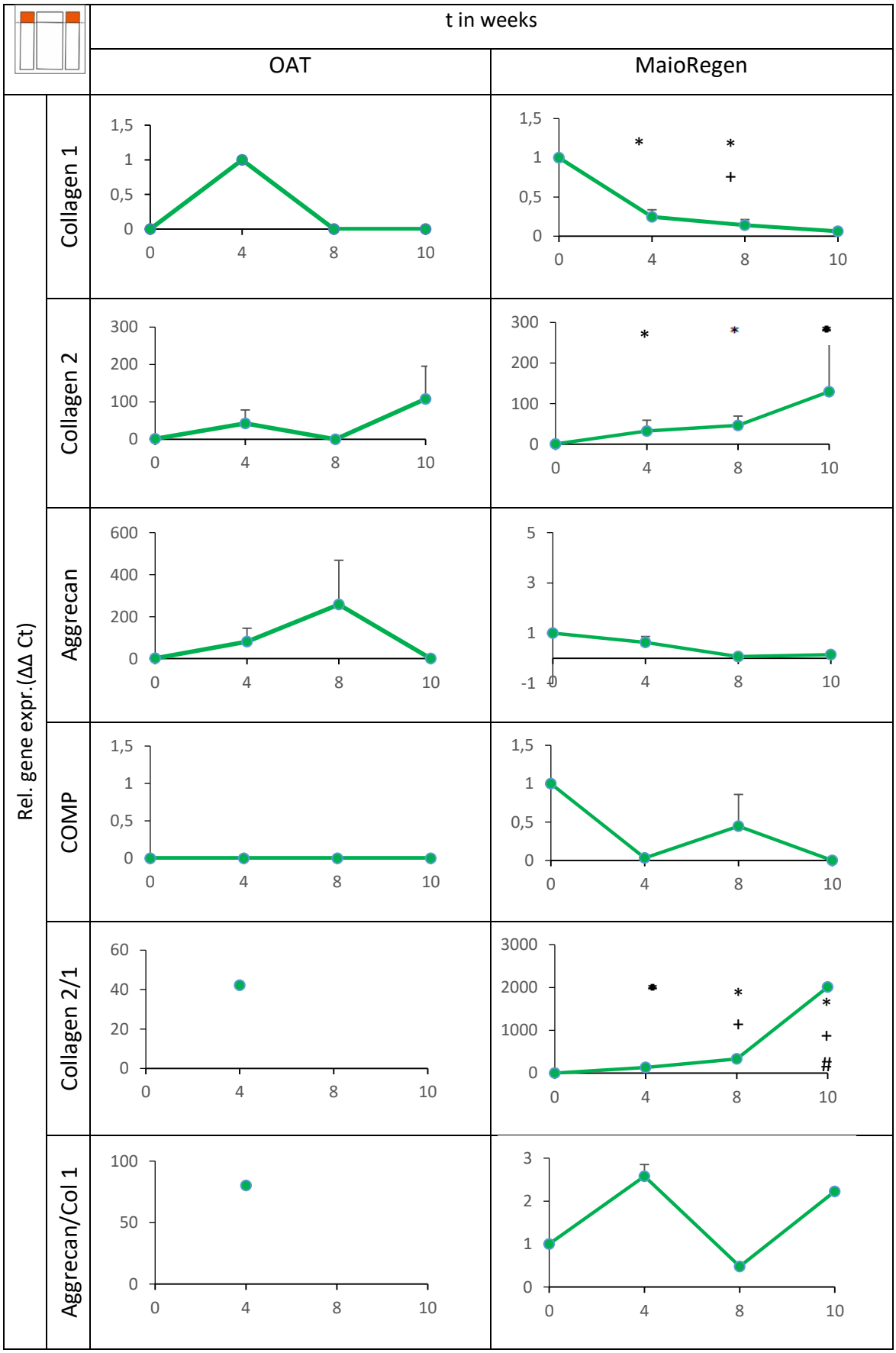

Figure 11: **Cartilage ring**; relative gene expression (ΔΔ Ct) of Collagen 1, Collagen 2, Aggrecan, and COMP in OAT and MaioRegen cultures (each n= 3) after 0, 4, 8 and 10 weeks. *p ≤ 0.05 vs. 0 weeks, +p ≤ 0.05 vs. 4 weeks, # p ≤ 0.05 vs. 8 weeks.

5.2.2 Cartilage ring (lysis buffer)

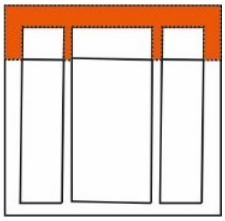

Collagen 1

Collagen 1 expression in the OAT group showed a transient peak at 4 and 8 weeks. In the MaioRegen group, collagen 1 expression was not detected at any time point (Fig. 12).

Collagen 2

In the OAT group, the expression of collagen 2 showed a constant level with a temporal maximum at 8 weeks. However, in the MaioRegen group the expression of collagen 2 continuously increased over time, reaching values 30-fold above baseline at 10 weeks (in analogy to the 100-fold increase over time in the corresponding cartilage rings; see Fig. 11).

Aggrecan

Aggrecan expression in the OAT group showed a maximum at 8 and 10 weeks, and also the aggrecan expression in the MaioRegen group continuously increased until 10 weeks (in parallel to the intense aggrecan signals at the surface of the cartilage ring and at the interface between the cartilage ring and the cartilaginous part of the MaioRegen scaffold; see Figure 9).

COMP

There was no expression of COMP in the OAT group. In the MaioRegen group, COMP expression increased to a peak at 8 and 10 weeks.

Collagen 2/1 ratio

In the OAT group, this ratio showed a decrease to very low values over time. As there was no collagen 1 expression in the MaioRegen group, this ratio was not informative.

Aggrecan/ Collagen 1

In the OAT group, this ratio continuously increased to a peak at 10 weeks. As explained above, this ratio was not informative for the MaioRegen group.

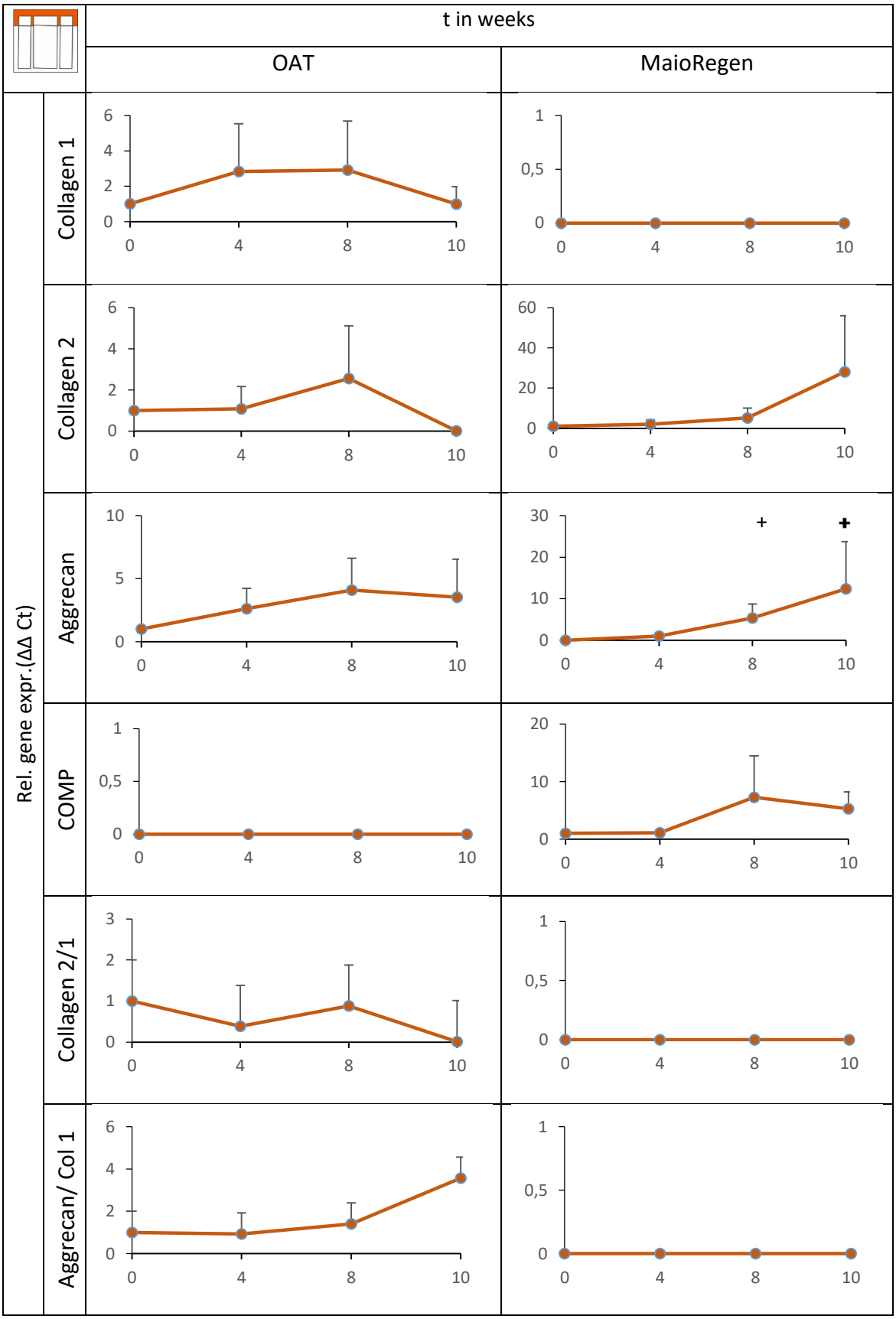

Figure 12: **Cartilage ring (lysis buffer)**; relative gene expression (ΔΔ Ct) of Collagen 1, Collagen 2, Aggrecan, and COMP in OAT and MaioRegen cultures (each n= 3) after 0, 4, 8 and 10 weeks. *p ≤ 0.05 vs. 0 weeks, +p ≤ 0.05 vs. 4 weeks, # p ≤ 0.05 vs. 8 weeks.

5.2.3 Bone ring

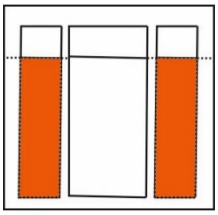

Collagen 1

In the OAT group, the gene expression of collagen 1 stayed at a plateau level until 4 weeks and then fell to non-detectable expression levels at 10 weeks. In the MaioRegen group, a significant peak was observed at 4 weeks (20-fold increase), which successively decreased to non-detectable values at 10 weeks.

Collagen 2

In the OAT group, collagen 2 expression showed a stepwise decrease to very low levels at 10 weeks. In the MaioRegen group, in contrast, collagen 2 expression showed a relative maximum after 4 weeks and thereafter returned to baseline levels.

Aggrecan

The expression of aggrecan in the OAT group continuously decreased to undetectable levels at 10 weeks. In the MaioRegen group, aggrecan expression showed a 2-fold increase until week 8 (in analogy to the increased aggrecan deposition observed in histology; Fig. 9).

COMP

In the OAT group, COMP was not detected at any time point. In the MaioRegen group, COMP expression increased 2-fold until 4 weeks and dropped thereafter.

Collagen 2/1 ratio

This ratio decreased to approx. ½ over time in the OAT group. In the MaioRegen group, this ratio showed a minimum at 4 and 8 weeks and returned to base line levels at 10 weeks.

Aggrecan/ Collagen 1

In the OAT group, this ratio remained nearly constant with a transient minimum after 4 weeks. In the MaioRegen group, this ratio drastically decreased beginning at 4 weeks to values much beneath baseline level.

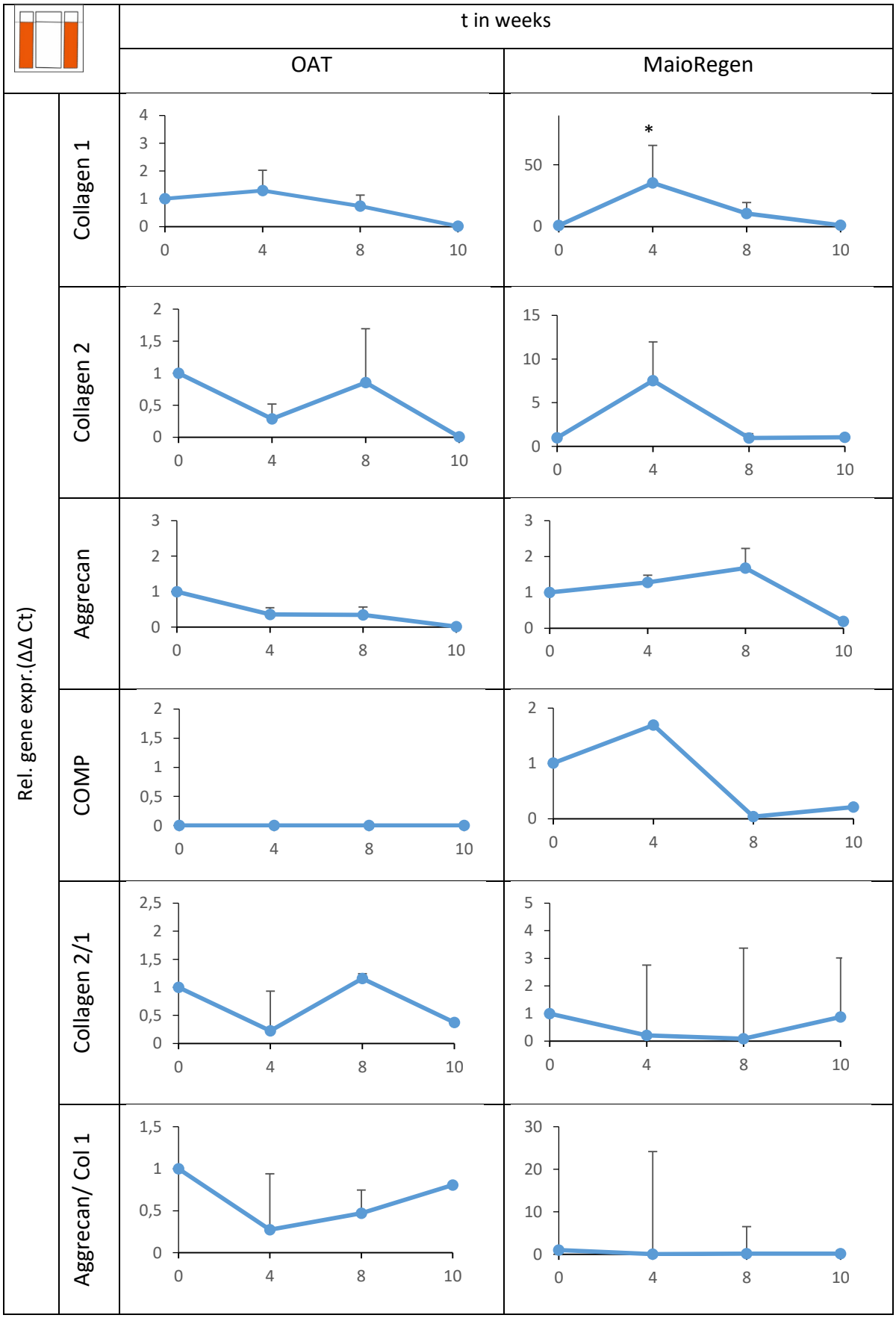

Figure 13: **Bone ring**; relative gene expression (ΔΔ Ct) of Collagen 1, Collagen 2, Aggrecan, and COMP in OAT and MaioRegen cultures (each n= 3) after 0, 4, 8 and 10 weeks. *p ≤ 0.05 vs. 0 weeks, +p ≤ 0.05 vs. 4 weeks, # p ≤ 0.05 vs. 8 weeks.

5.2.4 Bone ring (lysis buffer)

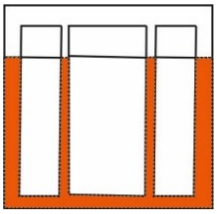

Collagen 1

While in the OAT group the expression of collagen 1 decreased from base line levels at 0 and 4 weeks to almost undetectable at 10 weeks, collagen 1 expression in the MaioRegen group rose to a 3-fold peak after 4 weeks and returned to baseline thereafter (Fig. 14; in both cases similar to the findings in the bone ring; see Fig. 13).

Collagen 2

Collagen 2 expression in the OAT group rose to a transient peak at 4 and 8 weeks and thereafter returned to baseline (similar to the bone ring; see Fig 13). In the MaioRegen group, there was no collagen 2 expression at any time point.

Aggrecan

Aggrecan expression showed a 400-fold peak at 4 weeks and a subsequent decline to baseline in the OAT group. In the MaioRegen group, there was again no mRNA expression.

COMP

There was no COMP expression in either the OAT or in the MaioRegen group.

Collagen 2/ 1 ratio

In the OAT group, this ratio steadily increased over time with a 3.5-fold maximum at 10 weeks. In the MaioRegen group, this ratio was not informative.

Aggrecan/ Collagen 1 ratio

In the OAT group, this ratio showed a 300-fold peak at 4 weeks and a subsequent decrease to values 200-fold above baseline. In the MaioRegen group, this ratio was again not informative.

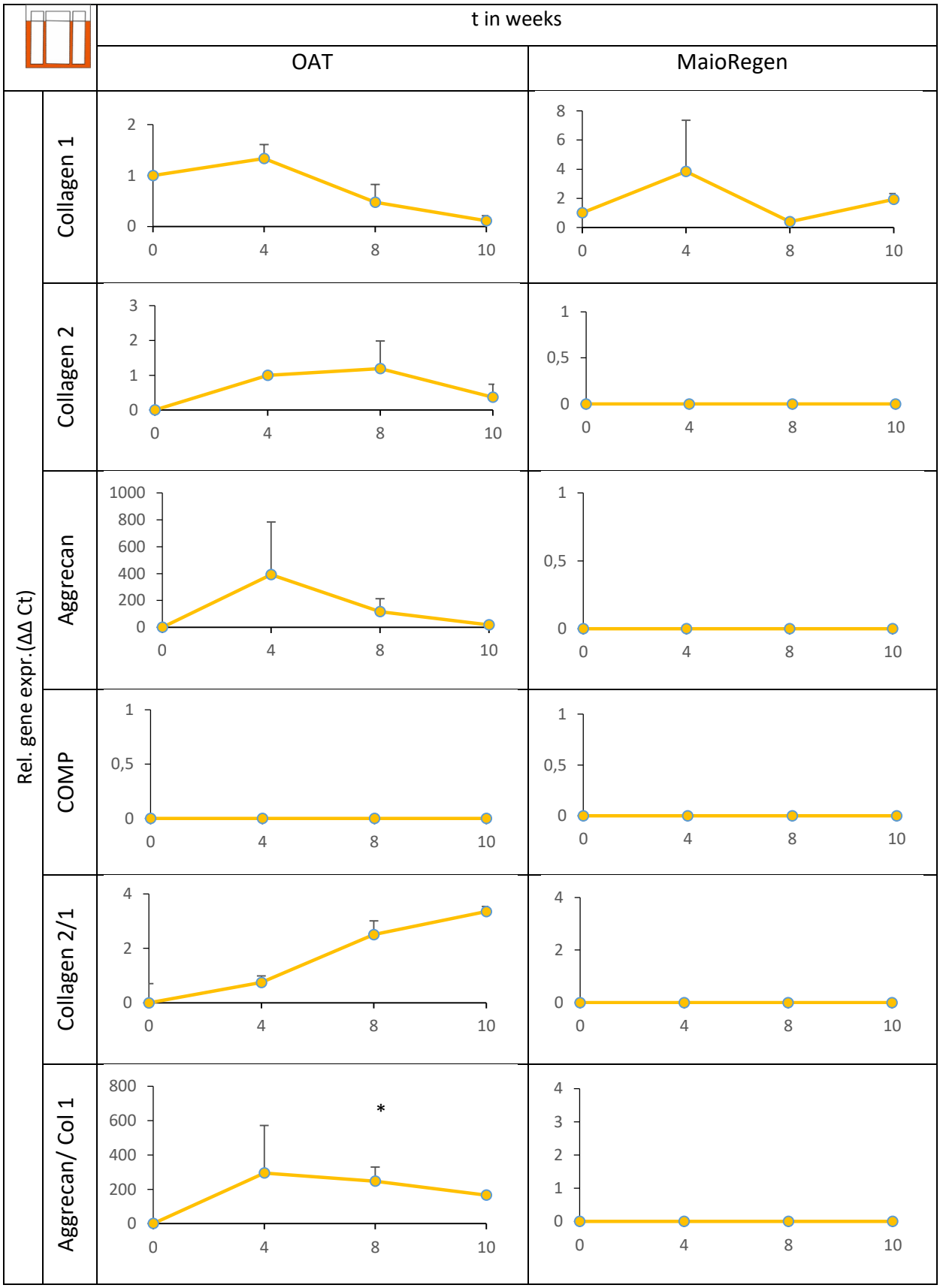

Figure 14: **Bone ring (lysis buffer)**; relative gene expression (ΔΔ Ct) of Collagen 1, Collagen 2, Aggrecan, and COMP in OAT and MaioRegen cultures (each n= 3) after 0, 4, 8 and 10 weeks. *p ≤ 0.05 vs. 0 weeks, +p ≤ 0.05 vs. 4 weeks, # p ≤ 0.05 vs. 8 weeks.

5.2.5 Implant cartilaginous part

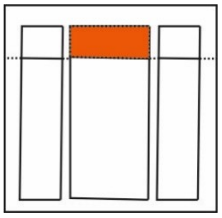

Collagen 1

In the OAT group, collagen mRNA showed a peak at 4 weeks and then decreased to a plateau above baseline levels. In the MaioRegen group, no collagen 1 expression was measured (Fig. 15).

Collagen 2

Collagen 2 expression was only detected at 8 weeks in the OAT group, but not in the MaioRegen group.

Aggrecan

Progressively increasing aggrecan expression was measured in the OAT group (20-fold above base-line at 10 weeks), while no expression was detected in the MaioRegen group.

COMP

COMP expression was not detected in either the OAT or in the MaioRegen group.

Collagen 2/ 1 ratio

In the OAT group, this ratio showed a peak value after 8 weeks. For the MaioRegen group, this ratio was not informative.

Aggrecan/ Collagen 1 ratio

In the OAT group, this ratio showed a continuous increase over time (Fig. 15; in analogy to the findings in the cartilage lysis buffer; see Fig 12). For the MaioRegen group, this ratio was again not informative.

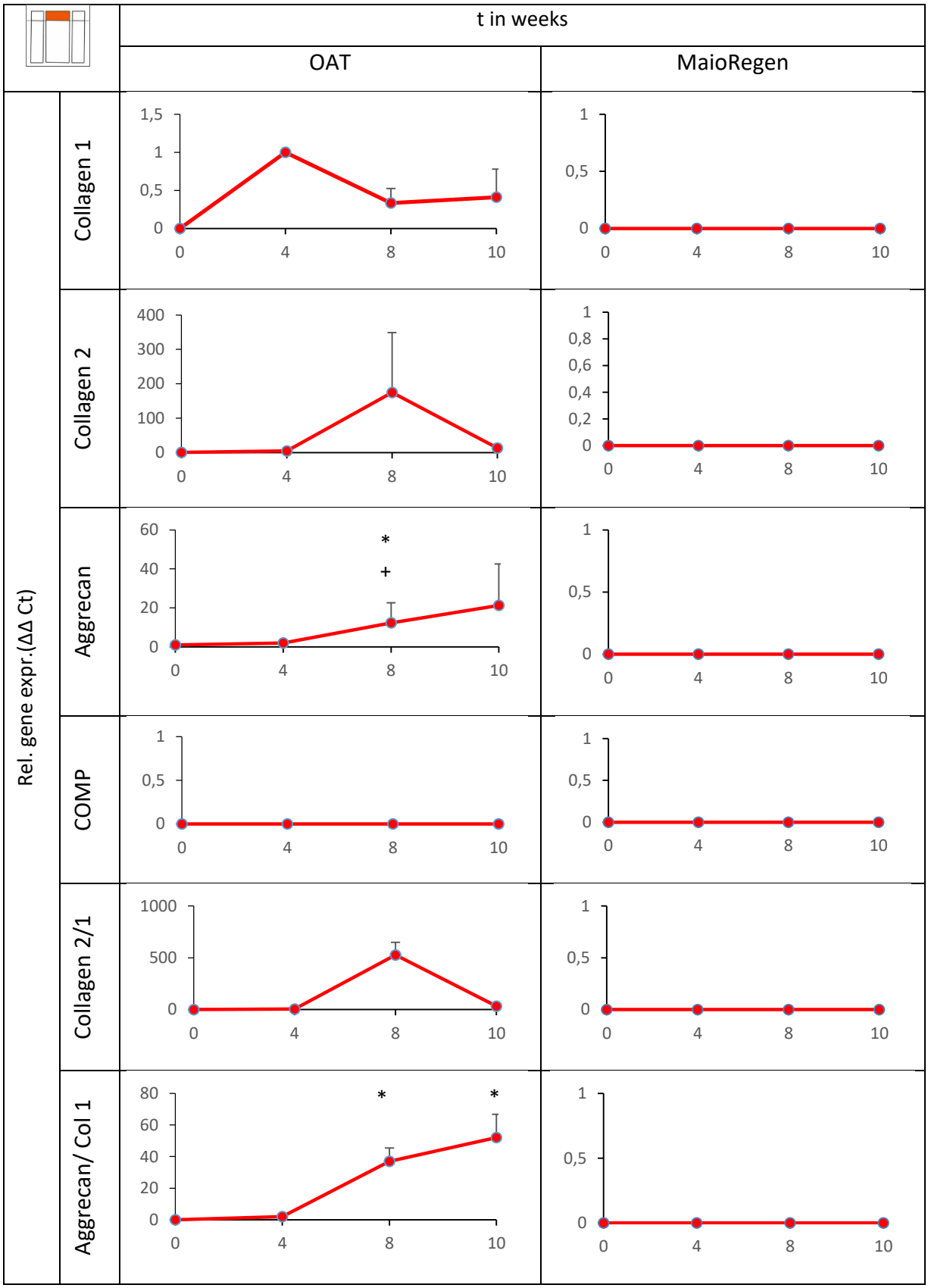

Figure 15: **Implant cartilaginous part**; relative gene expression (ΔΔ Ct) of Collagen 1, Collagen 2, Aggrecan, and COMP in OAT and MaioRegen cultures (each n= 3) after 0, 4, 8 and 10 weeks. *p ≤ 0.05 vs. 0 weeks, +p ≤ 0.05 vs. 4 weeks, # p ≤ 0.05 vs. 8 weeks.

5.2.6 Implant osseous part

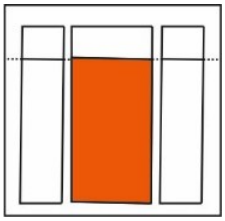

Collagen 1

The collagen 1 expression in the OAT group stayed at baseline levels throughout culture. In the MaioRegen group, expression showed a transient peak-value at 8 weeks (7.5-fold) and then decreased again (Fig. 16).

Collagen 2

The expression of collagen 2 in the OAT group showed a significant peak at 4 weeks (4-fold), followed by a decrease to expression values below baseline. In the MaioRegen group, the curve of collagen 2 expression peaked at 8 weeks with a more than 20-fold increase and thereafter decreased to levels above baseline.

Aggrecan

In the OAT group, aggrecan was expressed at constant levels with a transient maximum after 4 weeks (comparable to the collagen 2 expression). In the MaioRegen group, there was an increase of the aggrecan expression at 8 weeks and a subsequent return to baseline levels thereafter (comparable to the collagen 2 expression, but also to the collagen 1 expression).

COMP

There was no COMP expression in either the OAT group or the MaioRegen group.

Collagen 2/ 1 ratio

In the OAT group, this ratio showed a significant peak at 4 weeks, followed by a continuous decrease to values below baseline at 10 weeks. A similar peak was detected in the MaioRegen group at 8 weeks.

Aggrecan/ Collagen 1 ratio

In the OAT group, this ratio showed a significant maximum at 4 weeks, whereas the maximum in the MaioRegen group is reached at 8 weeks (Fig. 16).

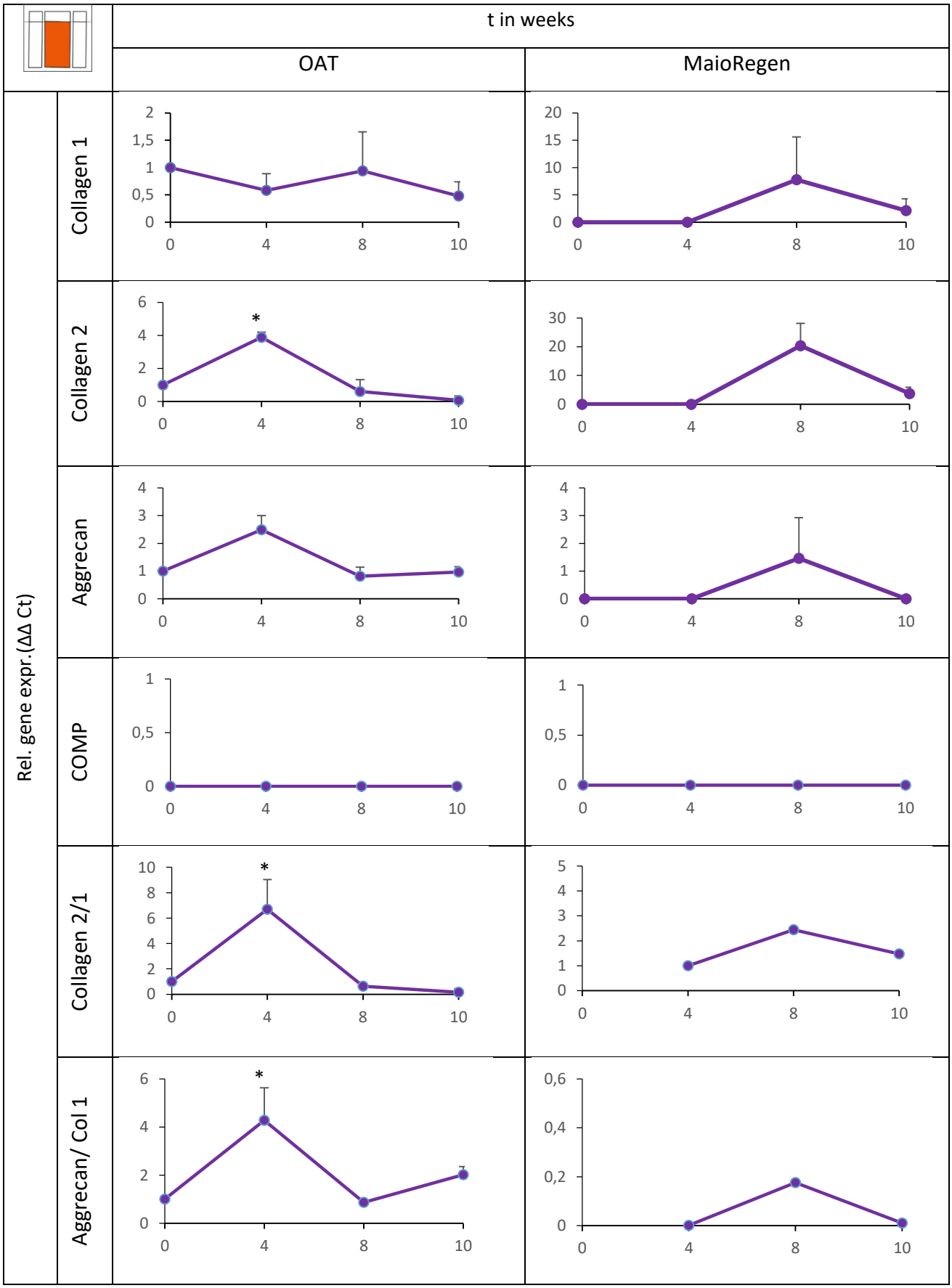

Figure 16: **Implant osseous part**; relative gene expression (ΔΔ Ct) of Collagen 1, Collagen 2, Aggrecan, and COMP in OAT and MaioRegen cultures (each n= 3) after 0, 4, 8 and 10 weeks. *p ≤ 0.05 vs. 0 weeks, +p ≤ 0.05 vs. 4 weeks, # p ≤ 0.05 vs. 8 weeks.

5.3 DMB Assay

For the DMB assay, the individual components of the osteochondral model [i.e., bone ring (and its lysis buffer preparation), cartilage ring, implant cartilaginous part, and implant osseous part] were subjected to separate measurements of their glycosaminoglycan (GAG) containment.

Cartilage Ring

In the cartilage rings of the OAT group, the content of GAG was largely constant over time (approx. 12 mg/g), with a minor peak after 8 weeks (19.7 mg/g). In the MaioRegen group, the GAG concentration was maintained at overall constant values (approx. 12.5 mg/g) with a transient minimum at 4 weeks.

Bone rings

In both the OAT and the MaioRegen group, the GAG concentration was almost constant over the whole culture period (approx. 24 mg/g).

Bone lysis buffer

In the OAT group, the concentration of GAGs increased steadily over time with a maximum at 10 weeks (8.6 mg/g). In the MaioRegen group, a maximum was measured after 4 weeks (8.5 mg/g), followed by concentrations above baseline.

Implant cartilaginous part

In the OAT group, there was a decrease in the GAG content detected over time (from 33.9 mg/g at 0 weeks; to10.1.mg/g at 10 weeks). In the MaioRegen group, however, constant values were observed (approx. 22 mg/g).

Implant osseous part

In the OAT group, increasing concentrations were observed with a peak at 8 weeks (max. 41.9 mg/g), that decreased thereafter (16.1 mg/g). In the MaioRegen group, GAG concentrations remained almost constant (approx. 17 mg/g).

There was no significant difference between OAT and MaioRegen for the GAG content in any component of the osteochondral model.

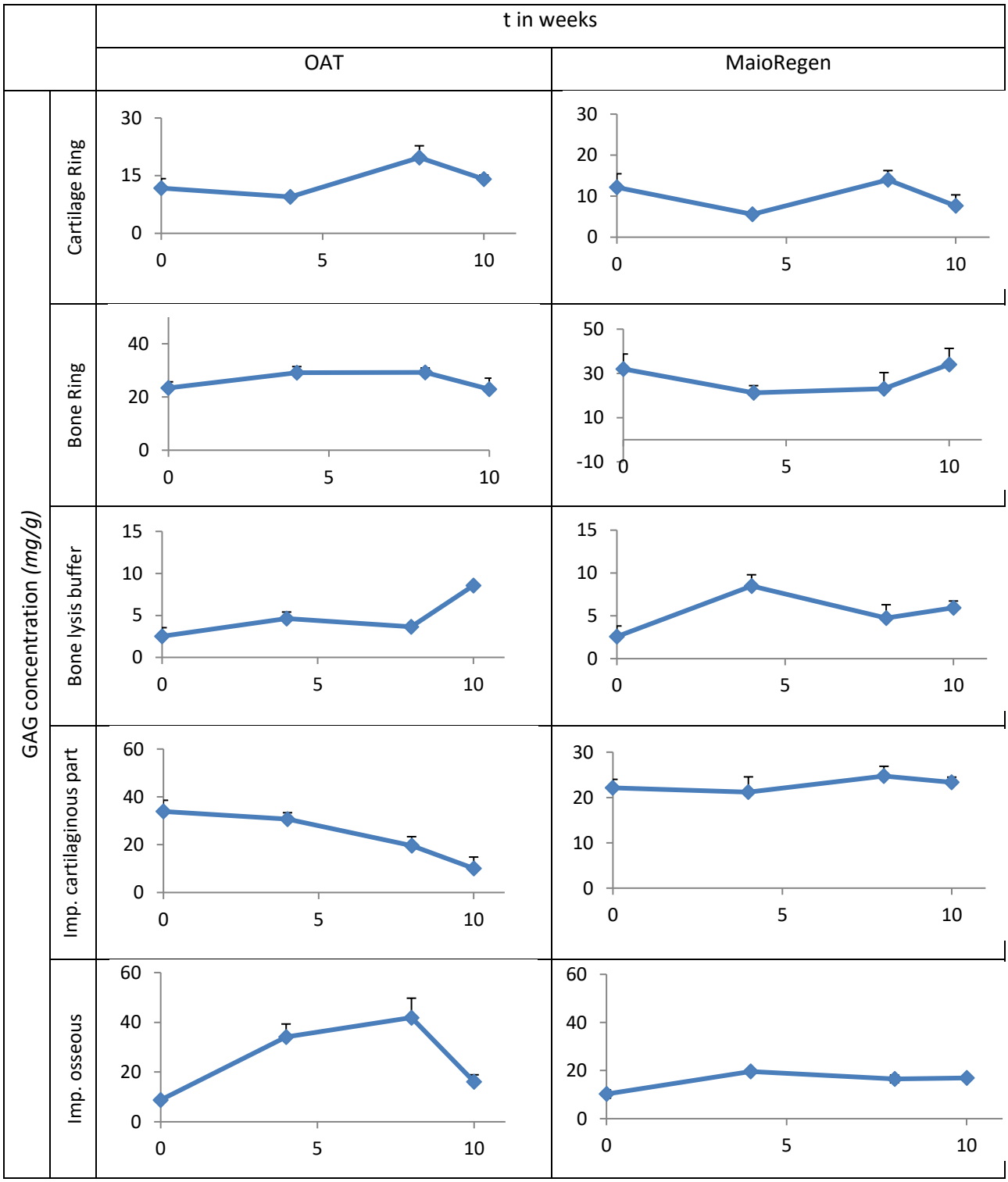

Figure 17: Shown are the GAG concentrations of either the OAT or the MaioRegen group over time (0, 4, 8, 10 wk) in **mg/g**. Data are presented as mean value ± SEM. *p ≤ 0.05 vs. 0 weeks, +p ≤ 0.05 vs. 4 weeks.

5.4 ELISA of the cell culture supernatants

Collagen 1: In the OAT group, the release of collagen 1 into the supernatants increased slightly during the first 4 weeks (from 13.0 µg/ml to 15.6 µg/ ml) and decreased in the time after to values below baseline (10.1µg/ml and 9.8 µg/ ml). In the MaioRegen group, there were different kinetics, with an increasing collagen 1 being release until 8 weeks (12.2 µg/ml) and a subsequent decrease (9.1 µg/ ml).

Collagen 2: In both the OAT and MaioRegen group, the concentrations of released collagen 2 remained constant with exception to a transient and significant minimum at 8 weeks (OAT: 109.7 µg/ml and MaioRegen: 71.0 µg/ml).

Aggrecan: In both groups, the aggrecan release into the supernatants showed constant values over time (approx. 60 ng/ml for OAT and MaioRegen).

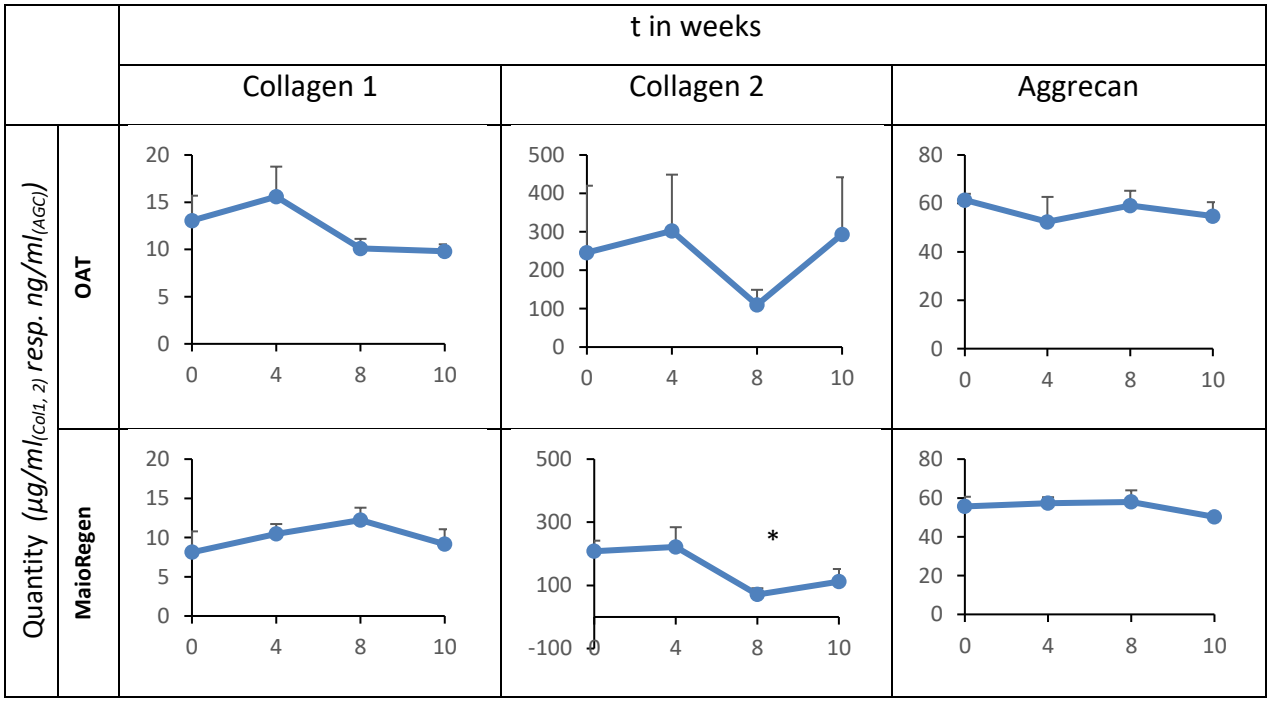

Figure 18: Quantification of collagen 1 (**µg/ml**), collagen 2 (**ng/ml**) and Aggrecan (**ng/ml**) concentrations in the supernatants of the cell cultures of OAT and MaioRegen®. Values are expressed as mean ± SEM; Standard error of the mean. *p ≤ 0.05 vs. 0 weeks, +p ≤ 0.05 vs. 4 weeks.

5.5 Biomechanical testing

Since the measurement of the push-out forces for the extrusion of the OAT implant resulted in values above the measurable range, valid measurements can only be reported for the MaioRegen group.

The largest push-out force (0.84 N) was detected at 4 weeks. This force decreased over time to very low values (0.23 N at 8 weeks; 0.17 N at 10 weeks).

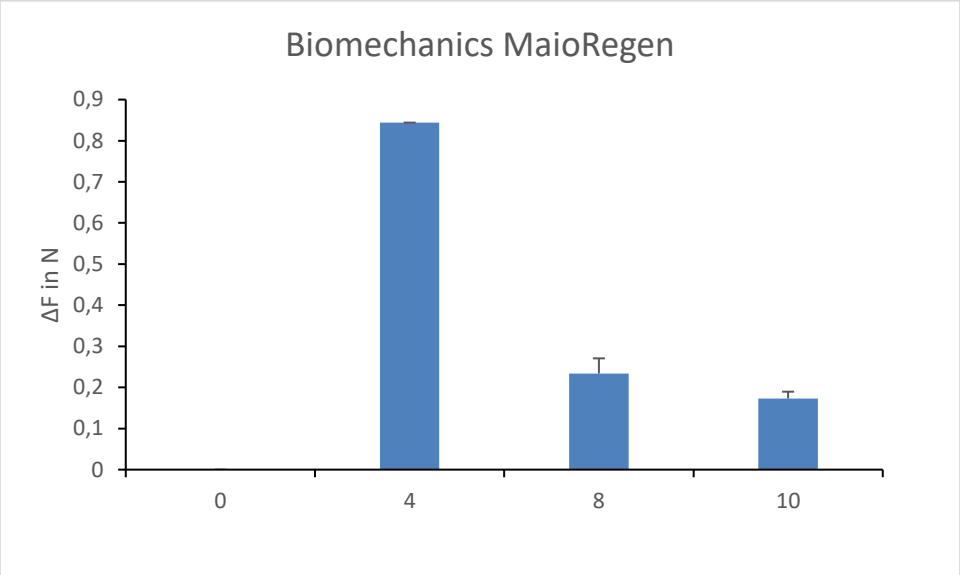

Figure 19: The force ΔF necessary to extrude the MaioRegen implant is shown for each time point of in vitro culture (0, 4, 8, and 10 weeks). Data are presented as means ± SEM.

6 DISCUSSION

6.1 Suitability of the new model

In this study, the OAT control implant and the cell-free, collagen-hydroxyapatite MaioRegen® scaffold were cultured for 0, 4, 8 and 10 weeks in bovine osteochondral cylinders and analyzed with regard to histology, gene expression, as well as biochemical and biomechanical features.

The present study represents the first report on a novel osteochondral model for the in vitro testing and analysis of diverse implants with clinical potential for the treatment of osteochondral defects. There are a number of advantages of this model: 1) it is readily available at low cost (slaughter house material); 2) it allows harvesting of up to 30 osteochondral cylinders from one bovine knee joint; 3) it is thus suitable for (semi) high-throughput studies, e.g. in an industrial setting, since large numbers of osteochondral cylinders can be cultured simultaneously with low demand on harvesting, handling, and (organ) culture; 4) the harvested osteochondral material initially shows intact tissue structures without structural alterations and largely maintains this integrity throughout culture for up to 10 weeks (without massive loss of proteoglycans or other matrix molecules); 5) it allows multi-technological and highly differential analysis for each of the involved tissue and material components of the new model.

All these points can be very challenging, if not impossible, when using human samples from patients suffering from osteoarthritis or other joint degenerative diseases. The involved tissue types survived 10 weeks of cell culture in this study without any signs of necrosis. They showed vital metabolic activity during the whole culture period. This observation is strengthened by an overall constant, long-term concentration of glycosaminoglycans in each of the tissue components (see Fig. 17).

On the other hand, some proteoglycan loss over time was observed in the cartilaginous parts of the osteochondral cylinder and the OAT control implant, possibly due to the well-known detachment of the lamina splendens (Sohn et al. 2002). Nevertheless, no clear signs of cartilage de-differentiation were observed either histologically or in gene expression analysis, again underlining the high vitality of the present in vitro culture model.

In particular, ‘callus-like’ bone formation around the OAT control implant and reintegration of the implant into the “host” osteochondral cylinder emphasized the vitality of the system. Similar tendencies were noted in a somewhat less complex

model system using exclusively cartilage cylinders (Dunzel et al. 2013). Also, large depositions of aggrecan were observed in the primarily cell-free MaioRegen scaffold. Thus, the model seems to provide optimal basic conditions to study the complex situation of osteochondral defect regeneration. It is therefore suitable for the analysis of diverse implants and their particular features, such as cell seeding and/or proliferation, matrix deposition, and successful tissue integration.

In the present study, the above-mentioned features were monitored using a combination of time-dependent surrogate parameters, e.g., structural and molecular (immuno) histological features, gene expression development, as well as the time course of matrix molecule content in the tissue/implant components and matrix release into the supernatant of the culture system. In comparison to previous studies investigating in vitro cartilage regeneration (Dunzel et al. 2013, Pretzel et al. 2013, Vinardell et al. 2009), the innovations and improvements of the present model are: 1) the use of an osteochondral host cylinder; 2) the application of a bone graft harvesting system well established in the clinical setting (Arthrex); and 3) the preparation of defect sizes that mimic the surface area of OATS cylinders in the clinical situation (approx. 0.2 cm^2). All these features serve to simulate the in vivo situation and thus to enhance the transferability to clinically relevant treatment approaches.

However, the limitations of this study are: 1) the use of bovine instead of human material with possible differences in structural, molecular, and biomechanical properties (Secretan et al. 2010); 2) the lack of regular blood supply and thus possibly insufficient long-term nutrition (Kuo et al. 2006); 3) the lack of biomechanical forces acting on the osteochondral cylinder and the implant during culture (Deschner et al. 2003); and 4) technical problems for the biomechanical testing of the OAT group (incarceration of the implant in the host cylinder).

6.2 Integrity of the osteochondral cylinders

In the OAT and the MaioRegen group, the cartilage ring of the host cylinder demonstrated chondrogenic differentiation during cell culture (Table 6). This is demonstrated by the detection of aggrecan in the matrix, aggrecan-positive cells on the cartilage surface, as well as increased gene expression for collagen 2 and aggrecan (see Fig. 11; Table 7). In addition, the glycosaminoglycan concentration of the cartilage ring remained on a stable level in the DMB assay, indicating constant net proteoglycan content in the cartilage ring (Fig. 17).

This net proteoglycan content of the cartilage ring in culture depends on at least 2 different and opposing factors. On one hand, there was considerable proteoglycan loss from the cartilage matrix, as indicated by a diminished staining in the Safranin-O and aggrecan staining and a continuous aggrecan release into the supernatant of both the OAT and MaioRegen cultures over the whole incubation period (approx. 60 ng/ml at all timepoints). However, an estimation of the proteoglycan content in the cartilage (approx. 6% w/w; approx. 3.2 mg in host cylinder and OAT implant) and the quantitative proteoglycan release into the culture supernatant (total of 10 ng/day and 560 ng in 8 weeks) indicated that at most 1-2% of the cartilage proteoglycan was released during culture (Muir 1978).

On the other hand, there were several indications for a local neo-synthesis of proteoglycans in the cultured cartilage (Aurich et al. 2005), e.g., aggrecan staining in the immediate vicinity of the chondrocytes and a redistribution of aggrecan molecules from a cohesive pattern to a multifocal mapping (Sternberg et al. 2013), increased collagen 2 and/or aggrecan gene expression in cartilage rings (and its lysis buffer preparation) in both implants groups, and a constant net glycosaminoglycan concentration in the tissue extracts of the cartilage ring. These findings suggest a vital balance of the proteoglycan molecules in the cartilage of the host cylinder and the OAT implant, which may also protect the collagen 2 in the cartilage against degradation by endogenous proteolytic enzymes (Pratta et al. 2003).

In comparison to previous studies using pure cartilage rings (Pretzel et al. 2013), there was only limited release of collagen 2 into the supernatant (approx. 250 ng/week). The likely reason for this difference is that in the present model there is only a very limited cartilage area artificially damaged by the preparation process. This is in agreement with very limited structural changes of the cartilage components in the current study, again supporting the concept of a vital and intact culture system.

Waldman et. al. showed that mechanical forces acting on the cartilage enhance the deposition of extracellular matrix proteins (Waldman et al. 2004). Thus, the lack of the mechanical stimulation may have had an impact on matrix deposition and release in the present study. As noted above, however, the very limited release of collagen 2 into the culture supernatant questions a major influence of the lacking biomechanical stimulation on the outcome of the experiments in the current study. In addition, a substantial increase of collagen 2 gene expression in the cartilage ring (and its lysis buffer preparation (Squires et al. 2003)), as well as an overall lack of fibroblastic

dedifferentiation (Tables 6 and 7) does not support a relevant influence of the missing biomechanical stimulation in the present study.

Tissue	Cartilage ring		Bone ring		Implant cartilaginous part		Implant osseous part		Cartilage surface*		Bone surface*	
	OAT	MR	OAT	MR	OAT	MR	OAT	MR	OAT	MR	OAT	MR
Tissue differentiation	↑	↑	↑	↑	↑		↓	↑	↑	↑	↓	↓
Cell migration	+	+	++	+	+	-	+	++	+	++	-	++

Table 6: Summary of principal histological changes. a) Tissue differentiation ↑ symbolizes a differentiation respective the primary tissue type of this site; ↓ indicates a de-differentiation to a tissue other than the primary tissue type, for the MaioRegen implant every type of tissue formation was counted as differentiation; b) Cell migration into the diverse compartments. - no cell migration, + moderate cell migration, ++ strong cell migration. *Cartilage/bone surface represents the histological equivalent to the term cartilage/bone lysis buffer used above; MR = MaioRegen

In analogy to the cartilage rings, the bone rings showed a similar behavior in the OAT and the MaioRegen group. Thus, the bone rings showed an extreme high vitality, which is based on the following features: 1) no histological observed necrosis or tissue degradation; 2) an almost complete closure of the osseous gap in the case of the OAT group and a substantial bone regeneration at the edge of the bone ring around the MaioRegen implant (Fig. 7); and 3) a transient decrease of the collagen 2/1 and aggrecan/ collagen 1 ratios (indicating conserved bone differentiation over time; Tables 6 and 7). In addition, proteoglycan deposition into the bone ring was observed histologically, with one focus on the immediate vicinity of the implant (Fig. 8). In combination with the above mentioned decrease of the gene expression ratios, this may reflect the attempt of the bone to regenerate via callus-like, enchondral tissue formation, most likely in response to the artificial fracture/trauma set by the harvesting technique (Cvetkovic et al. 2015). Further evidence for this hypothesis is provided by the collagen 2 and aggrecan gene expression kinetics with an initial increase and a late decrease (Fig. 13), as this is typical for long term enchondral ossification through primary de-differentiation with subsequent bone differentiation (Bucholz 2002, Park et al. 2015).

Furthermore substantial and overall constant collagen 1 release into the culture supernatants was detected (Fig. 18), while collagen 1 expression showed to be decreasing over time in the both the OAT and the MaioRegen group. Considering the histological intactness of the bone ring, release and limited neo synthesis are of minor

importance for the integrity of the bone rings, as the other above-mentioned processes are predominant this tissues vitality and integrity.

6.3 Matrix formation of the implants

In the cartilaginous part of the OAT implant, no structural major changes, i.e. massive tissue degradation, tissue de-differentiation, or gap closure between implant and ring, were observed. The latter as an expression of insufficient regeneration capacity is a well-known phenomenon of cartilage due to its complex structure and bradytrophic nutrition (Siebert et al. 2001, Obradovic et al. 2001).

In analogy to the situation in the bone ring, the osseous part of the implant showed large proteoglycan depositions starting at 4 weeks of culture (Fig. 8) that resulted in increasing glycosaminoglycan contents. In addition, gene expression of collagen 1, 2 and aggrecan initially increased and decreased thereafter (Fig. 16). This again, supported by overall decreasing collagen 2/1 and aggrecan/collagen 1 ratios, supports the hypothesis of callus-like tissue formation in this osteochondral model (Schnabel et al. 2002) and gives evidence for cross-talk between the implant and its “host” osteochondral cylinder. Similar observations regarding gap closure and cross-talk were made in animal models as well as in the clinical setting (Woelfle et al. 2013, Richter et al. 2015, Siebert et al. 2001).

In comparison to the bone ring, in the osseous part of the implant nutrients have to diffuse over longer distances, therefore metabolism may show somewhat different kinetics (Burke und Kelly 2012). In this study, this accounts for large proteoglycan depositions, which are more intense and cohesive in the implant than in the bone ring of both the OAT and the MaioRegen group. This suggests not only a high vitality of this tissue but also massive matrix formation in the implant.

In the collagen-enriched top lay of the MaioRegen scaffold no cell migration was observed, rather degradation and dissolution dominated this structure. This is in contrast to experimental in vivo studies that were carried out previously (Kon et al. 2010). Considering the impressive density of this layer may reason for its impermeability for cell migration (Pretzel et al. 2013). The dissolution of this layer is most likely caused by both, its solubility and its weak attachment to the underlying layer. Thus, large flakes shifted off during culture. Yet it remains questionable if joints treated with MaioRegen scaffolds that were arthroscopically examined in a second look biopsy showed to be very soft because the top layer had dissolved (Brix et al. 2016).

	OAT		MaioRegen	
	Collagen 2/1	AGC/ Col 1	Collagen 2/1	AGC/ Col 1
Cartilage rings	↑	↑	↑	↑
Cartilage (rings) lysis buffer	↓	↑	↑	↑
Bone rings	↓	↓	↓	↓
Bone (rings) lysis buffer	↑	↑	↓	↓
Implant cartilaginous part	↑	↑	-	-
Implant osseous part	↓	↓	↑	↑

Table 7: Comparison of diverse gene expression patterns across tissues and groups. Indicated are the overall tendencies over time of (de-)differentiation ratios (Collagen 2/1 and AGC/ Col 1). Generally, in cartilaginous tissue increasing ratios signify differentiation, while the opposite is true in osseous tissue.

In contrast, the lower and hydroxyapatite containing layer of the MaioRegen scaffold showed to be an attractive location for cell migration. Histologically large aggrecan and proteoglycan depositions were detected in this layer. In addition, gene expression for collagen 1, 2 and aggrecan showed a peak after 8 weeks. This late maximum is most likely caused by an initial de-differentiation and subsequent re-differentiation of the mRNA expression in cells that had migrated into the scaffold – a phenomenon well-known from monolayer cell culture that is eventually transferred into a 3D culture (Darling und Athanasiou 2005, Kaps et al. 2004).

Comparing the metabolic activities of this layer to the one of the osseous part of the OAT, it seems likely that callus-like tissue formation and enchondral ossification at an early stage is taking place here as well (Christensen et al. 2015, Filardo et al. 2013).

Although the MaioRegen scaffold dissolved and the gap between implant and “host” osteochondral cylinder enlarged, cross-talk was observed as the bone ring showed bone formation on the edge neighboring the implant.

Furthermore, in pure chondral in vitro models it often has been shown that chondrocytes are the responsible cell type for the measured gene expression in scaffolds (Pretzel et al. 2013). However, in the present model, several tissue components may be the origin of cell emigration, thus diverse cell types may emigrate. In both the OAT and the MaioRegen group, cells that had emigrated onto the cartilage showed cartilage-like gene expression patterns (Fig. 12). Cells that emigrated onto the bone ring showed cartilaginous gene expression patterns as well in the OAT group. However, in the MaioRegen group only collagen 1 gene expression was detected (Fig. 14). Thus, it can be hypothesized that 1) through cross-talk MaioRegen may limit the emigration of cartilaginous cells onto the bone or 2) that it enhances the

emigration/differentiation of cells with fibrous origin or capacity (Vinardell et al. 2009, Im 2015). However, this specific detail can be answered only partially by the analysis of the cartilage and/or bone lysis buffer and may therefore be subject of further research.

Although the osseous part of the scaffold is capable of stabilizing cells of a fibrocartilaginous phenotype, there is no evidence for a lateral bonding with biomechanical impact at any time, which is explained by histological evidence for the scaffold's dissolution. Thus, decreasing resistances in biomechanical testing and questionable clinical results of the MaioRegen implant can be reasoned on a molecular level (Brix et al. 2016, Christensen et al. 2015).

6.4 Tenor of this study and prospects for the clinical use

This study is of great interest as it: 1) showed a novel, stable osteochondral culture system; 2) identified structural and molecular reactions of the analyzed tissue components (differentiating vs. de-differentiating processes, matrix deposition, cell migration, tissue integration; Tables 6 and 7); 3) found reasons for the impaired clinical performance of the MaioRegen scaffold on a molecular level and 3) demonstrated high tissue-integrative properties of OATs.

Clinical efforts to repair damaged articular cartilage currently face major obstacles due to limited intrinsic repair capacity of the tissue and unsuccessful biological interventions. This shows the need for better therapeutic strategies (Caldwell und Wang 2015). In the present in vitro model, the gold standard for osteochondral repair, which is the OAT, proved highly suitable for osseous regeneration (Kadakia und Espinosa 2013).

The cell-free MaioRegen scaffold showed tissue-adapting properties such as cell migration, extracellular protein deposition, and biocompatibility without any signs of toxicity. These findings are in accordance with previously gathered in vivo data (Kon et al. 2009, Kon et al. 2010). However, recent clinical studies noted similar critical points of this scaffold such as poor osteochondral integration, alleged partial dissolution and a somewhat weak lateral bonding capacity (Brix et al. 2016). As these clinical findings can be strengthened by the presented experimental in vitro data, further research has to be initiated in order to assess the general clinical applicability of this construct.

7 CONCLUSION

The described model is suitable for the in-vitro investigation of osteochondral defects and their appropriate treatment via natural transplants or specifically tissue-engineered implants. In addition, it has a quasi-unlimited availability and is of reproducible quality. Furthermore, it is cost-effective and provides a broad spectrum of molecular and mechanical techniques for consecutive analysis. Consequently, large data contribute to the comprehension of this complex system, which is crucial for the final assessment of the implant being investigated.

In the present study, the osteochondral integrative abilities of the MaioRegen® scaffold and the osteochondral healing responses of OATs were compared. In both groups, cross-talk between the implant and the osteochondral rings were observed, indicating vigorous processes in the system.

In this study, the clinically widely established OAT technique proofed its osteochondral healing response on a bio-structural level. Therefore, this group could be considered as a to-be-established standardized control group for future studies in this setting. This is of interest, as pre-clinical, standardized in vitro testing will be of increasing importance for future product licensing (European Medicines Agency 2009).

In contrast to the OAT, the MaioRegen scaffold's structural long-term stability has to be questioned, as it histologically seemed to lose its density, dissolving in the course of the experiment. Therefore, with respect to recent clinical data (Christensen et al. 2015, Brix et al. 2016), the scaffold has not only to be used with caution in the clinical context but also has to be object to further studies because different clinical studies found contrary results (Berruto et al. 2014, Filardo et al. 2013, Kon et al. 2012).

This demonstrates the demand for further research concerning MaioRegen in particular and osteochondral regeneration in general, which is of common interest for the individually affected patient and the contributors of the health care system.

8 REFERENCES

Aurich M, Squires GR, Reiner A, Mollenhauer JA, Kuettner KE, Poole AR, Cole AA. 2005. Differential matrix degradation and turnover in early cartilage lesions of human knee and ankle joints. Arthritis Rheum, 52 (1):112-119.

Bedi A, Lynch EB, Sibilsky Enselman ER, Davis ME, Dewolf PD, Makki TA, Kelly BT, Larson CM, Henning PT, Mendias CL. 2013. Elevation in circulating biomarkers of cartilage damage and inflammation in athletes with femoroacetabular impingement. Am J Sports Med, 41 (11):2585-2590.

Behery O, Siston RA, Harris JD, Flanigan DC. 2014. Treatment of cartilage defects of the knee: expanding on the existing algorithm. Clin J Sport Med, 24 (1):21-30.

Berruto M, Delcogliano M, de Caro F, Carimati G, Uboldi F, Ferrua P, Ziveri G, De Biase CF. 2014. Treatment of Large Knee Osteochondral Lesions With a Biomimetic Scaffold: Results of a Multicenter Study of 49 Patients at 2-Year Follow-up. Am J Sports Med, 42 (7):1607-1617.

Bobic V. 1999. [Autologous osteo-chondral grafts in the management of articular cartilage lesions]. Orthopade, 28 (1):19-25.

Brighton CT, Kitajima T, Hunt RM. 1984. Zonal analysis of cytoplasmic components of articular cartilage chondrocytes. Arthritis Rheum, 27 (11):1290-1299.

Brix M, Kaipel M, Kellner R, Schreiner M, Apprich S, Boszotta H, Windhager R, Domayer S, Trattnig S. 2016. Successful osteoconduction but limited cartilage tissue quality following osteochondral repair by a cell-free multilayered nano-composite scaffold at the knee. Int Orthop.

Broom ND, Marra DL. 1985. New structural concepts of articular cartilage demonstrated with a physical model. Connect Tissue Res, 14 (1):1-8.

Bucholz RW. 2002. Nonallograft osteoconductive bone graft substitutes. Clin Orthop Relat Res, (395):44-52.

Buckwalter JA. 1997. Were the Hunter brothers wrong? Can surgical treatment repair articular cartilage? Iowa Orthop J, 17:1-13.

Burke DP, Kelly DJ. 2012. Substrate stiffness and oxygen as regulators of stem cell differentiation during skeletal tissue regeneration: a mechanobiological model. PLoS One, 7 (7):e40737.

Caldwell KL, Wang J. 2015. Cell-based articular cartilage repair: the link between development and regeneration. Osteoarthritis Cartilage, 23 (3):351-362.

Chandrasekhar S, Esterman MA, Hoffman HA. 1987. Microdetermination of proteoglycans and glycosaminoglycans in the presence of guanidine hydrochloride. Anal Biochem, 161 (1):103-108.

Christensen BB, Foldager CB, Jensen J, Jensen NC, Lind M. 2015. Poor osteochondral repair by a biomimetic collagen scaffold: 1- to 3-year clinical and radiological follow-up. Knee Surg Sports Traumatol Arthrosc.

Cvetkovic VJ, Najdanovic JG, Vukelic-Nikolic MD, Stojanovic S, Najman SJ. 2015. Osteogenic potential of in vitro osteo-induced adipose-derived mesenchymal stem cells combined with platelet-rich plasma in an ectopic model. Int Orthop, 39 (11):2173-2180.

Darling EM, Athanasiou KA. 2005. Rapid phenotypic changes in passaged articular chondrocyte subpopulations. J Orthop Res, 23 (2):425-432.

Delcogliano M, de Caro F, Scaravella E, Ziveri G, De Biase CF, Marotta D, Marenghi P, Delcogliano A. 2014. Use of innovative biomimetic scaffold in the treatment for large osteochondral lesions of the knee. Knee Surg Sports Traumatol Arthrosc, 22 (6):1260-1269.

Demoor M, Ollitrault D, Gomez-Leduc T, Bouyoucef M, Hervieu M, Fabre H, Lafont J, Denoix JM, Audigie F, Mallein-Gerin F, Legendre F, Galera P. 2014. Cartilage tissue engineering: molecular control of chondrocyte differentiation for proper cartilage matrix reconstruction. Biochim Biophys Acta, 1840 (8):2414-2440.

Deschner J, Hofman CR, Piesco NP, Agarwal S. 2003. Signal transduction by mechanical strain in chondrocytes. Curr Opin Clin Nutr Metab Care, 6 (3):289-293.

Dewan AK, Gibson MA, Elisseeff JH, Trice ME. 2014. Evolution of autologous chondrocyte repair and comparison to other cartilage repair techniques. Biomed Res Int, 2014:272481.

Dunzel A, Rudiger T, Pretzel D, Kopsch V, Endres M, Kaps C, Fohr P, Burgkart RH, Linss S, Kinne RW. 2013. [The bovine cartilage punch model: a tool for the in vitro analysis of biomaterials and cartilage regeneration]. Orthopade, 42 (4):254-261.

European Medicines Agency E. 2009. In-vitro cultured chondrocyte containing products for cartilage repair of the knee.

Fiedler T. 2014. Eignung von bakterieller Nanocellulose als Knorpelersatzmaterial – molekularbiologische und proteinbiochemische Analysen im in vitro Knorpelstanzenmodell. University thesis:51.

Filardo G, Kon E, Di Martino A, Busacca M, Altadonna G, Marcacci M. 2013. Treatment of knee osteochondritis dissecans with a cell-free biomimetic osteochondral scaffold: clinical and imaging evaluation at 2-year follow-up. Am J Sports Med, 41 (8):1786-1793.

Gillogly SD, Wheeler KS. 2015. Autologous Chondrocyte Implantation With Collagen Membrane. Sports Med Arthrosc, 23 (3):118-124.

Gobbi A, Chaurasia S, Karnatzikos G, Nakamura N. 2015. Matrix-Induced Autologous Chondrocyte Implantation versus Multipotent Stem Cells for the Treatment of Large Patellofemoral Chondral Lesions: A Nonrandomized Prospective Trial. Cartilage, 6 (2):82-97.

Goldring MB, Goldring SR. 2007. Osteoarthritis. J Cell Physiol, 213 (3):626-634.

Goymann V. 1999. [Abrasion arthroplasty]. Orthopade, 28 (1):11-18.

Gross JM. 2009. Musculoskeletal Examination. (3):p. 17-20.

Hart DJ, Doyle DV, Spector TD. 1999. Incidence and risk factors for radiographic knee osteoarthritis in middle-aged women: the Chingford Study. Arthritis Rheum, 42 (1):17-24.

Hayes DW, Jr., Brower RL, John KJ. 2001. Articular cartilage. Anatomy, injury, and repair. Clin Podiatr Med Surg, 18 (1):35-53.

Hedlund H, Mengarelli-Widholm S, Reinholt FP, Svensson O. 1993. Stereologic studies on collagen in bovine articular cartilage. APMIS, 101 (2):133-140.

Im GI. 2015. Endogenous Cartilage Repair by Recruitment of Stem Cells. Tissue Eng Part B Rev.

Jay GD, Waller KA. 2014. The biology of lubricin: near frictionless joint motion. Matrix Biol, 39:17-24.

Kadakia AR, Espinosa N. 2013. Why allograft reconstruction for osteochondral lesion of the talus? The osteochondral autograft transfer system seemed to work quite well. Foot Ankle Clin, 18 (1):89-112.

Kaps C, Fuchs S, Endres M, Vetterlein S, Krenn V, Perka C, Sittinger M. 2004. [Molecular characterization of tissue-engineered articular chondrocyte transplants based on resorbable polymer fleece]. Orthopade, 33 (1):76-85.

Khan IM, Gilbert SJ, Singhrao SK, Duance VC, Archer CW. 2008. Cartilage integration: evaluation of the reasons for failure of integration during cartilage repair. A review. Eur Cell Mater, 16:26-39.

Kleemann RU, Krocker D, Cedraro A, Tuischer J, Duda GN. 2005. Altered cartilage mechanics and histology in knee osteoarthritis: relation to clinical assessment (ICRS Grade). Osteoarthritis Cartilage, 13 (11):958-963.

Kon E, Delcogliano M, Filardo G, Altadonna G, Marcacci M. 2009. Novel nano-composite multi-layered biomaterial for the treatment of multifocal degenerative cartilage lesions. Knee Surg Sports Traumatol Arthrosc, 17 (11):1312-1315.

Kon E, Vannini F, Buda R, Filardo G, Cavallo M, Ruffilli A, Nanni M, Di Martino A, Marcacci M, Giannini S. 2012. How to treat osteochondritis dissecans of the knee: surgical techniques and new trends: AAOS exhibit selection. J Bone Joint Surg Am, 94 (1):e1(1-8).

Kon E, Delcogliano M, Filardo G, Fini M, Giavaresi G, Francioli S, Martin I, Pressato D, Arcangeli E, Quarto R, Sandri M, Marcacci M. 2010. Orderly osteochondral regeneration in a sheep model using a novel nano-composite multilayered biomaterial. J Orthop Res, 28 (1):116-124.

Konig A, Kirschner S. 2003. [Long-term results in total knee arthroplasty]. Orthopade, 32 (6):516-526.

Kuo CK, Li WJ, Mauck RL, Tuan RS. 2006. Cartilage tissue engineering: its potential and uses. Curr Opin Rheumatol, 18 (1):64-73.

Lim EH, Sardinha JP, Myers S. 2014. Nanotechnology biomimetic cartilage regenerative scaffolds. Arch Plast Surg, 41 (3):231-240.

Lynch TS, Patel RM, Benedick A, Amin NH, Jones MH, Miniaci A. 2015. Systematic review of autogenous osteochondral transplant outcomes. Arthroscopy, 31 (4):746-754.

Martinek V, Ueblacker P, Imhoff AB. 2003. Current concepts of gene therapy and cartilage repair. J Bone Joint Surg Br, 85 (6):782-788.

Mesallati T, Buckley CT, Kelly DJ. 2015. Engineering cartilaginous grafts using chondrocyte-laden hydrogels supported by a superficial layer of stem cells. J Tissue Eng Regen Med.

Mollon B, Kandel R, Chahal J, Theodoropoulos J. 2013. The clinical status of cartilage tissue regeneration in humans. Osteoarthritis Cartilage, 21 (12):1824-1833.

Mubarak SJ, Carroll NC. 1981. Juvenile osteochondritis dissecans of the knee: etiology. Clin Orthop Relat Res, (157):200-211.

Muir H. 1978. Proteoglycans of cartilage. J Clin Pathol Suppl (R Coll Pathol), 12:67-81.

Muir H. 1995. The chondrocyte, architect of cartilage. Biomechanics, structure, function and molecular biology of cartilage matrix macromolecules. Bioessays, 17 (12):1039-1048.

O'Driscoll SW, Keeley FW, Salter RB. 1986. The chondrogenic potential of free autogenous periosteal grafts for biological resurfacing of major full-thickness defects in joint surfaces under the influence of continuous passive motion. An experimental investigation in the rabbit. J Bone Joint Surg Am, 68 (7):1017-1035.

Obradovic B, Martin I, Padera RF, Treppo S, Freed LE, Vunjak-Novakovic G. 2001. Integration of engineered cartilage. J Orthop Res, 19 (6):1089-1097.

Oussedik S, Tsitskaris K, Parker D. 2015. Treatment of articular cartilage lesions of the knee by microfracture or autologous chondrocyte implantation: a systematic review. Arthroscopy, 31 (4):732-744.

Park KW, Yun YP, Kim SE, Song HR. 2015. The Effect of Alendronate Loaded Biphasic Calcium Phosphate Scaffolds on Bone Regeneration in a Rat Tibial Defect Model. Int J Mol Sci, 16 (11):26738-26753.

Poole CA. 1997. Articular cartilage chondrons: form, function and failure. J Anat, 191 (Pt 1):1-13.

Pratta MA, Yao W, Decicco C, Tortorella MD, Liu RQ, Copeland RA, Magolda R, Newton RC, Trzaskos JM, Arner EC. 2003. Aggrecan protects cartilage collagen from proteolytic cleavage. J Biol Chem, 278 (46):45539-45545.

Pretzel D, Linss S, Ahrem H, Endres M, Kaps C, Klemm D, Kinne RW. 2013. A novel in vitro bovine cartilage punch model for assessing the regeneration of focal cartilage defects with biocompatible bacterial nanocellulose. Arthritis Res Ther, 15 (3):R59.

Richter DL, Schenck RC, Jr., Wascher DC, Treme G. 2015. Knee Articular Cartilage Repair and Restoration Techniques: A Review of the Literature. Sports Health.

Roth V, Mow VC. 1980. The intrinsic tensile behavior of the matrix of bovine articular cartilage and its variation with age. J Bone Joint Surg Am, 62 (7):1102-1117.

Schinhan M, Gruber M, Vavken P, Dorotka R, Samouh L, Chiari C, Gruebl-Barabas R, Nehrer S. 2012. Critical-size defect induces unicompartmental osteoarthritis in a stable ovine knee. J Orthop Res, 30 (2):214-220.

Schnabel M, Marlovits S, Eckhoff G, Fichtel I, Gotzen L, Vecsei V, Schlegel J. 2002. Dedifferentiation-associated changes in morphology and gene expression in primary human articular chondrocytes in cell culture. Osteoarthritis Cartilage, 10 (1):62-70.

Secretan C, Bagnall KM, Jomha NM. 2010. Effects of introducing cultured human chondrocytes into a human articular cartilage explant model. Cell Tissue Res, 339 (2):421-427.

Shakibaei M, Csaki C, Rahmanzadeh M, Putz R. 2008. [Interaction between human chondrocytes and extracellular matrix in vitro: a contribution to autologous chondrocyte transplantation]. Orthopade, 37 (5):440-447.

Siebert CH, Miltner O, Schneider U, Wahner T, Koch S, Niedhart C. 2001. [Healing of osteochondral transplants--animal experiment studies using a sheep model]. Z Orthop Ihre Grenzgeb, 139 (5):382-386.

Sohn DH, Lottman LM, Lum LY, Kim SG, Pedowitz RA, Coutts RD, Sah RL. 2002. Effect of gravity on localization of chondrocytes implanted in cartilage defects. Clin Orthop Relat Res, (394):254-262.

Squires GR, Okouneff S, Ionescu M, Poole AR. 2003. The pathobiology of focal lesion development in aging human articular cartilage and molecular matrix changes characteristic of osteoarthritis. Arthritis Rheum, 48 (5):1261-1270.

Sternberg H, Kidd J, Murai JT, Jiang J, Rinon A, Erickson IE, Funk WD, Wang Q, Chapman KB, Vangsness CT, Jr., West MD. 2013. Seven diverse human embryonic stem cell-derived chondrogenic clonal embryonic progenitor cell lines display site-specific cell fates. Regen Med, 8 (2):125-144.

Triche R, Mandelbaum BR. 2013. Overview of cartilage biology and new trends in cartilage stimulation. Foot Ankle Clin, 18 (1):1-12.

Tuan RS, Chen AF, Klatt BA. 2013. Cartilage regeneration. J Am Acad Orthop Surg, 21 (5):303-311.

Ulrich-Vinther M, Maloney MD, Schwarz EM, Rosier R, O'Keefe RJ. 2003. Articular cartilage biology. J Am Acad Orthop Surg, 11 (6):421-430.

Vinardell T, Thorpe SD, Buckley CT, Kelly DJ. 2009. Chondrogenesis and integration of mesenchymal stem cells within an in vitro cartilage defect repair model. Ann Biomed Eng, 37 (12):2556-2565.

Wakitani S, Goto T, Pineda SJ, Young RG, Mansour JM, Caplan AI, Goldberg VM. 1994. Mesenchymal cell-based repair of large, full-thickness defects of articular cartilage. J Bone Joint Surg Am, 76 (4):579-592.

Waldman SD, Spiteri CG, Grynpas MD, Pilliar RM, Kandel RA. 2004. Long-term intermittent compressive stimulation improves the composition and mechanical properties of tissue-engineered cartilage. Tissue Eng, 10 (9-10):1323-1331.

Woelfle JV, Reichel H, Nelitz M. 2013. Indications and limitations of osteochondral autologous transplantation in osteochondritis dissecans of the talus. Knee Surg Sports Traumatol Arthrosc, 21 (8):1925-1930.

Appendix

Materialtables:

Tables:

Figures:

Danksagung

Hiermit möchte ich mich bei der Arbeitsgruppe Experimentelle Rheumatologie unter Leitung von Herrn Professor Dr. med. habil. R.W. Kinne für die Bereitstellung des Labors und die fachliche, beratende Unterstützung zu allen Zeitpunkten der Arbeit herzlich bedanken.

Großer Dank gilt auch meinen Eltern, Freunden und geistig nahestehenden Personen die mich in der ideellen Realisierung dieses Projekts unterstützt haben.

Ehrenwörtliche Erklärung

Hiermit erkläre ich, dass mir die Promotionsordnung der Medizinischen Fakultät der Friedrich-Schiller-Universität bekannt ist,

ich die Dissertation selbst angefertigt habe und alle von mir benutzten Hilfsmittel, persönlichen Mitteilungen und Quellen in meiner Arbeit angegeben sind,

mich folgende Personen bei der Auswahl und Auswertung des Materials sowie bei der Herstellung des Manuskripts unterstützt haben: Prof. Dr. med. R. W. Kinne,

die Hilfe eines Promotionsberaters nicht in Anspruch genommen wurde und dass Dritte weder unmittelbar noch mittelbar geldwerte Leistungen von mir für Arbeiten erhalten haben, die im Zusammenhang mit dem Inhalt der vorgelegten Dissertation stehen,

dass ich die Dissertation noch nicht als Prüfungsarbeit für eine staatliche oder andere wissenschaftliche Prüfung eingereicht habe und

dass ich die gleiche, eine in wesentlichen Teilen ähnliche oder eine andere Abhandlung nicht bei einer anderen Hochschule als Dissertation eingereicht habe.

Ort, Datum Unterschrift des Verfassers